



Fundamentals and applications of enzyme powered micro/nano-motors

Hao Yuan^a, Xiaoxia Liu^a, Liying Wang^a, Xing Ma^{a,b,c,*}

^a Flexible Printed Electronic Technology Center and School of Materials Science and Engineering, Harbin Institute of Technology (Shenzhen), Shenzhen, 518055, China

^b Shenzhen Bay Laboratory, No. 9 Duxue Road, Shenzhen, 518055, China

^c Key Laboratory of Microsystems and Microstructures Manufacturing, Harbin Institute of Technology, Harbin, Heilongjiang, 150001, China

ARTICLE INFO

Keywords:

Micro/nano-motors
Enzymes
Bio-catalytic reactions
Active motion
Self-propulsion mechanism

ABSTRACT

Micro/nanomotors (MNM)s are miniaturized machines that can convert many kinds of energy into mechanical motion. Over the past decades, a variety of driving mechanisms have been developed, which have greatly extended the application scenarios of MNMs. Enzymes exist in natural organisms which can convert chemical energy into mechanical force. It is an innovative attempt to utilize enzymes as biocatalyst providing driving force for MNMs. The fuels for enzymatic reactions are biofriendly as compared to traditional counterparts, which makes enzyme-powered micro/nanomotors (EMNMs) of great value in biomedical field for their nature of biocompatibility. Until now, EMNMs with various shapes can be propelled by catalase, urease and many others. Also, they can be endowed with multiple functionalities to accomplish on-demand tasks. Herein, combined with the development process of EMNMs, we are committed to present a comprehensive understanding of EMNMs, including their types, propelling principles, and potential applications. In this review, we will introduce single enzyme that can be used as motor, enzyme powered molecule motors and other micro/nano-architectures. The fundamental mechanism of energy conversion process of EMNMs and crucial factors that affect their movement behavior will be discussed. The current progress of proof-of-concept applications of EMNMs will also be elaborated in detail. At last, we will summarize and prospect the opportunities and challenges that EMNMs will face in their future development.

1. Introduction

“There is plenty of room at the bottom” which was presented by Richard Feynman at the California Institute of Technology’s annual meeting of Physics in 1959. The talk is considered to be the genesis of nanotechnology. His speech has been a great inspiration to scientific community, including invention of miniaturized machines scaling down to micro/nano-scale. The sci-fi film *Fancy Voyage* tells such a story of navigating a medical micro/nano-ship in human blood vessels to perform vascular surgery, which has been a long cherished scientific dream for the field of micro/nano-motors (MNM)s. MNMs are kinds of miniaturized devices or structures that can convert chemical or other forms of energy into mechanical force that propel the movement of themselves. Like intelligent robots at macro-scale, MNMs can perform fine operations in complex environment. Due to their characteristics of small size and autonomous movement, they demonstrate promising prospects in the fields of drug delivery [1], minimally invasive surgery [2,3], biochemical sensing [4], and environmental remediation [5,6].

Because of their rich structure and propulsion mechanism, MNMs can be applied in many fields. In biomedicine, MNMs can move to narrow space to perform minimally invasive surgery. In terms of environmental applications, MNMs can remove pollutants by degradation or adsorption with enhanced efficiency by micro-stirring. The development of MNMs is of great interest and benefit for scientific and engineering communities. However, with size of the machines scaling down, due to the low Reynolds number condition viscosity would become dominating factor and hinder the movement of MNMs. In addition, Brownian motion would also bring challenges to the control of the motors’ motion behavior. So, external propelling mechanisms different from those of macro-scale machines are needed to achieve active propulsion [7]. Over the past decades many publications have reported the development of MNMs’ propulsion mechanisms. MNMs can be propelled by chemistry reactions [8], light [9], ultrasound [10], magnetic fields [11], electric fields [12], etc. Variety of propelling strategies enriches the scenarios of the MNMs’ movement environment, which in return enable MNMs to perform many more functions.

* Corresponding author. Flexible Printed Electronic Technology Center and School of Materials Science and Engineering, Harbin Institute of Technology (Shenzhen), Shenzhen, 518055, China.

E-mail address: maxing@hit.edu.cn (X. Ma).

<https://doi.org/10.1016/j.bioactmat.2020.11.022>

Received 23 September 2020; Received in revised form 12 November 2020; Accepted 13 November 2020

2452-199X/© 2020 The Authors. Production and hosting by Elsevier B.V. on behalf of KeAi Communications Co., Ltd. This is an open access article under the CC

BY-NC-ND license (<http://creativecommons.org/licenses/by-nc-nd/4.0/>).

Enzyme is an important biocatalyst, which has high specificity and catalytic efficiency. Enzyme is one kind of proteins which is ubiquitous in organism and intrinsically biocompatible taking account of their natural origin. Enzymes triggered biocatalytic reactions that provide energy for most biological activities of living cells, which usually take place under mild conditions in physiological environment. Furthermore, most MNMs are prepared by non-degradable inorganic materials or biotoxic materials, which is a great limit to biomedical applications. However, enzyme-powered micro/nanomotors (EMNMs) based on naturally originated bioproteins of enzymes show apparent advantages for biomedical purpose as compared to conventional MNMs. Due to the good biocompatibility of enzymes, biologically available chemical fuel and the mild enzymatic reaction conditions, EMNMs thus have attracted considerable attentions in recent years.

With the advance of MNMs, EMNMs have made great progress in their propelling strategies, application scenarios, and choice of constructing materials. Scientists initially discovered that enzymes move autonomously as active motors themselves [13]. Enzymes have been proposed to produce motion by a range of debated mechanisms including configurational change, thermal effect, phoresis effect, chemocoustic effect, etc. Enzymes can be immobilized onto artificially synthesized architectures, and propel these micro/nano-structures by different propulsion mechanisms, e.g. self-electrophoresis and bubble propulsion. EMNMs can be propelled by a single enzyme such as catalase, urease, glucose oxidase (GOx), etc. And they can also be propelled by multiple enzymes, among which enzymatic cascade reaction is used to propel motors, such as the widely reported combination of catalase and glucose oxidase. Biodegradable EMNMs [14] and motors that can move under physiological concentrations have also been developed [15]. EMNMs can be used for drug delivery, biosensing, environmental remediation, etc., thus exhibiting considerable potentials in practical applications. However, it is also noticed that the biological nature and biocatalytic characteristic of enzymes have brought extra concerns on the performance of enzymatic motors. Therefore, scientists have studied the propelling mechanisms and influencing factors of EMNMs, in order to provide in-depth theoretical and fundamental understanding on this research topic, which is crucial for the future development of EMNMs.

This review aims to give a comprehensive introduction of EMNMs. We will introduce different types of enzymatic motors, including single enzyme motor, molecule motors, and artificial motors propelled by different enzymes. The propulsion strategies and fundamental mechanisms on EMNMs, as well as crucial factors affecting their motion behavior will be discussed. The applications of EMNMs will also be elaborated in detail in hope of inspiring possible applications in other engineering fields. Finally, we summarize and prospect the opportunities and challenges that EMNMs will face in future development, which gives suggestions on the research directions that of scientific interest and significance for the community.

2. Types and propulsion strategies of EMNMs

2.1. Molecule motors and enzymes as motors

In 1773, Italian scientist L. Spallanzani did an interesting experiment in which an eagle swallowed an iron cage with meat. After taken out, the meat in the cage disappeared, which proved the existence of enzymes in the stomach of the eagle. Enzymes are proteins based biocatalysts produced by living cells with high specificity for substrates and catalytic efficiency. Up to now, scientists have revealed considerable knowledge about the fundamental chemistry of enzymes, including their catalytic mechanism and kinetics of enzymatic reactions. With regarding to their mechanical motion behavior, researchers have proved that enzymes can move autonomously in the presence of substrates, which make themselves classified as EMNMs. In addition, there are molecular machines made of proteins in living organisms that can move at molecular scale by consuming energy from enzymatic decomposition of substances.

Because of their small size and ability to move autonomously powered by enzymatic reactions, they are also regarded as EMNMs here. Both of self-propelled single enzyme and molecular motor are natural, non-synthesized EMNMs.

Molecular motors exist in cells with wide varieties. They participate in a series of important life activities such as cytoplasmic transport, muscle contraction, and ATP synthesis. Myosin moves along actin filaments [16,17], while dynein and kinesin move along microtubules [18]. These three types of molecular motors are called linear molecular motor. ATP synthase is kind of rotating molecular motor. The four types of molecular motors are all named ATPases, because they rely on ATP decomposition to release chemical energy to achieve their motion functions (Fig. 1A) [19]. The main function of myosin is to provide muscle contraction. Because myosin exists in different cells and tissues, there are many kinds of myosins. Since myosin has ATPase activity, it can decompose ATP at low ionic strength to achieve the vibration of its head on actin filaments, then the whole myosin is stretched forward, thus achieving the movement of myosin [16,17]. Dynein participates in important life activities such as cell mitosis and energy supply of mitochondria. The energy of dynein movement also comes from the decomposition of ATP. Kinesin is similar to dynein in movement on microtubules, but experiments have shown that kinesin movement is directional along the positive or negative poles of microtubules [19]. ATP synthase is widely present in mitochondrial inner membrane, chloroplast and other organelles, participating in ATP synthesis and decomposition. ATP synthase [20] (Fig. 1B) consists of F_0 embedded in the cell membrane and F_1 in the head. F_0 and F_1 are consist of different numbers of subunits. During the synthesis and decomposition of ATP, F_0 or F_1 rotates due to the directional flow of chemical substances in cells, which drives the rotation of another part. The direction of rotation during the synthesis and decomposition is opposite. Noji and co-workers first observed the rotation of ATP synthase in 1997 [21,22]. In addition, Montemagno and co-workers found that ATP synthase can propel the movement of microspheres modified with ATP synthase [23].

In addition to the ATPase that acts as molecular motors in organism, catalase, urease and some other enzymes exhibiting enhanced diffusion phenomenon in present of substrates have been regarded as motors themselves. Sen's group studied the enhanced diffusion trend of urease in the presence of substrates and they found that the diffusion coefficient of urease is strongly related to substrate concentration [24] (Fig. 1C). The group also utilized a microfluidic device to generate substrate concentration gradient and found that catalase and urease would accumulate to the substrate of a higher concentration [25] (Fig. 1D). Glucose oxidase was used to generate hydrogen peroxide by bio-catalytically decomposition of glucose, which would further induce catalase migration by chemotaxis. Then, the group demonstrated this phenomenon in subsequent work that DNA polymerase would accumulate toward the direction of high concentrations of nucleotides and cofactors [26]. And a micro/nanopump was prepared by immobilizing DNA polymerase on the substrate. Besides, Granick's group observed the movement of urease and acetylcholinesterase using superresolution microscopy. They found that the diffusion coefficient of enzymes increases with substrate concentration. Moreover, they first proposed the concept of enzyme anti-chemotaxis and confirmed that catalytic enzymes are active matter in later research [27]. The catalytic reaction of enzymes will promote its movement. Scientists have been trying to find direct evidences of enhanced diffusion of enzyme motors.

2.2. Single enzymatic reaction propelled EMNMs

Molecular motors and enzymes like catalase or urease are naturally exist in animals and plants. Although these enzymes can move automatically as motors themselves, they have limited applications due to lack of functionality and difficulty in the control of their motion behavior. Obviously, these naturally existing EMNMs are not "smart" enough to achieve complex operation or accomplish on-demand task. By

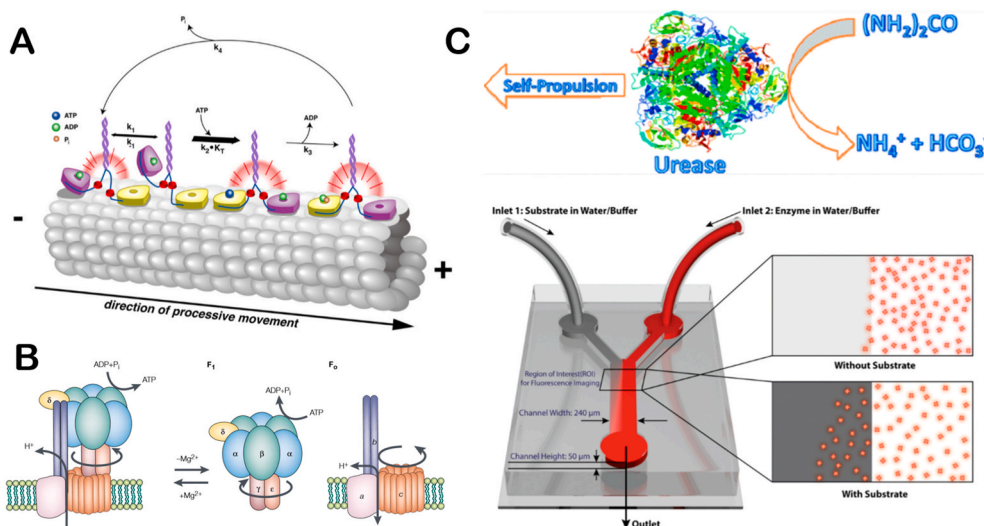


Fig. 1. The illustration of molecule motors and single enzyme motors (A) Schematic depiction of the kinesin mechanochemical cycle. Reproduced with permission from ref 18. Copyright 2009, PNAS. (B) Structure of ATP synthase. Reproduced with permission from ref 20. Copyright 2001, Nature. (C) Schematic depiction of urease self-actuation. Reproduced with permission from ref 24. Copyright 2010, American Chemical Society. (D) Schematic illustration chemotactic of enzyme molecules. Reproduced with permission from ref 25. Copyright 2013, American Chemical Society.

loading enzymes onto artificial micro/nanostructures like spherical particles or tubes, to prepare artificially synthesized EMNMs which are propelled by the catalysis of enzymes and can perform multiple functions within complex environment.

2.2.1. Catalase powered EMNMs

Encouraged by the widely explored catalytic system of Pt/H₂O₂ which generates strong movement thrust by decomposition of hydrogen peroxide, catalase powered motors initially became the early model of enzymatic motors. Sánchez and co-workers modified the interior of the rolling-up microtubes with catalase by linker molecules of 3-mercaptopropionic acid (3-MPA) [28] (Fig. 2A). The motor can move in lower concentrations of hydrogen peroxide (1.5 wt%) at 10 body length/s

compared with 1 body length/s for the Pt-based counterpart, which proved their improved catalytic efficiency of enzymatic motors. Later, Orozco and co-workers prepared a PEDOT/Au-catalase tubular motor using electrodeposition method [29] (Fig. 2B). The motor can detect water quality by detecting the change of motor's velocity which is correlated to the activity of catalase in present of pollution. Recent years, Fu and co-workers assembled catalase into microtubules in multiple layers through programmed DNA hybridization [30]. It can move at speed of 51 μm/s in 0.25% hydrogen peroxide. The authors used the motors for DNA detection.

It is commonly known that hydrogen peroxide is toxic to cells, and the generation of bubbles *in vivo* will also cause adverse effects to human bodies. High concentration of H₂O₂ fuel would apparently limit the

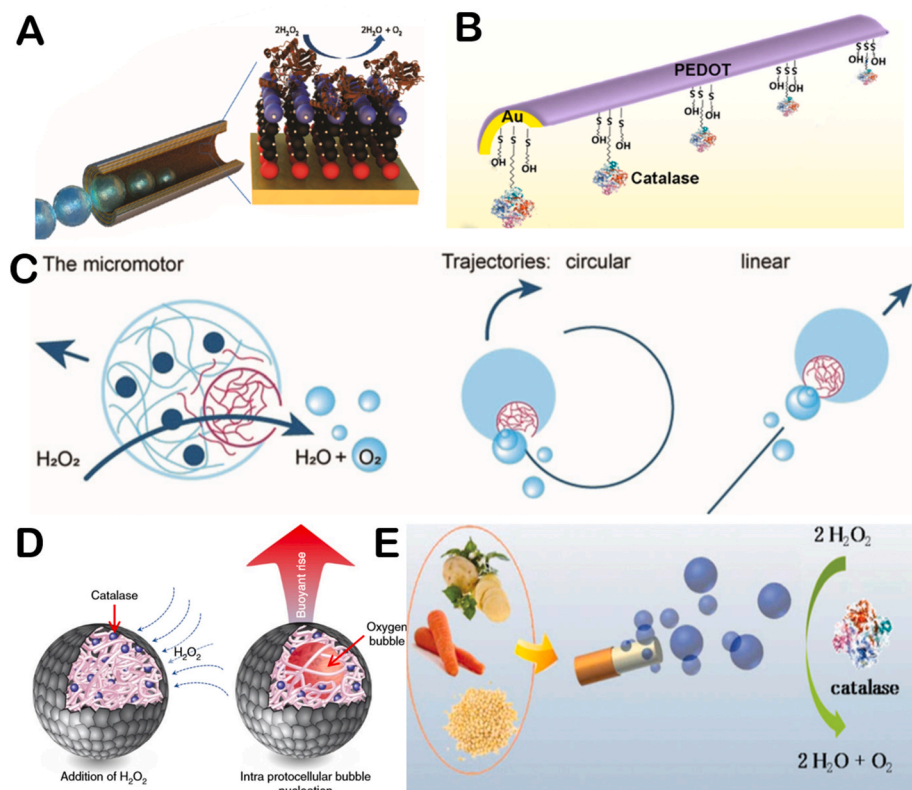


Fig. 2. The illustration of catalase powered EMNMs (A) Catalase propelled tubular motor. Reproduced with permission from ref 28. Copyright 2010, American Chemical Society. (B) PEDOT/Au-catalase tubular motor capable of testing water quality. Reproduced with permission from ref 29. Copyright 2012, American Chemical Society. (C) Schematic representation of catalase powered EMNMs which decomposes hydrogen peroxide into propelling oxygen. Reproduced with permission from ref 32. Copyright 2018, Wiley. (D) Buoyant motility in organoclay/DNA microcapsules. Reproduced with permission from ref 36. Copyright 2018, Nature. (E) Schematic illustration of the plant-tissue based Janus motors. Reproduced with permission from ref 40. Copyright 2013, The Royal Society of Chemistry.

potential biomedical applications of the catalase powered EMNMs [31]. Thus, it is of great significance to develop EMNMs that can move in a lower concentration of hydrogen peroxide. Until now, the development of catalase powered tubular EMNMs have made it possible to be fueled with quite low hydrogen peroxide concentration. However, the current concentration of H_2O_2 used in research is still highly toxic to living cells, which although hinders the wide exploration of catalase powered EMNMs in biomedical field, but holds more possibilities and feasibilities in other fields such as biochemical sensing or environmental sedimentation.

In addition to tubular EMNMs introduced above, catalase was also used to power micro/nano particles based spherical motors due to their simple preparation methods and larger output. Wilson's group prepared an asymmetric catalase powered EMNMs using microfluidic chips [32] (Fig. 2C). The motor is propelled by catalase encapsulated in microgroove. And the roughness of microgroove's surface can be adjusted by high molecular weight dextran, which can regulate the motor's speed. This work enabled the flexibility and controllability on the motor's rotational and translational speed. Recently, the group prepared an ultrasmall stomatocyte polymersomes, the size of which is around 150 nm [33]. The stomatocyte motor was prepared by squeezing the flexible polymersomes with PEG. By adding catalase to the solution, catalase could be encapsulated inside the motor. Due to its tiny size, it has stronger tissue penetration capability in biomedical applications. Besides, based on the fact that most motors were constructed of metallic or inorganic structures, the group prepared the first degradable catalase powered EMNM made of organic materials. Aiming at potential applications in nanomedicine, smaller size of motors is required [14]. Ma and co-workers prepared a Janus mesoporous silica motor with the size of about 100 nm using chemical synthesis method combined with electron-beam evaporation [34]. The diffusion coefficient of the motor at low hydrogen peroxide concentration (below 3 wt%) is increased by 150% compared to its intrinsic Brownian motion. Recently, Li and co-workers used a complex chemical synthesis method to prepare a single-molecule nanomotor less than 100 nm based on molecular bottlebrush (MBB), which has a tadpole-like asymmetry. It can overcome Brownian motion and move in ultra-low concentration of hydrogen peroxide (0.006 wt%) of high viscous environment [35].

In addition to traditional capability of directional self-propulsion, researchers developed catalase powered EMNMs that achieved other form of motion behavior as well as additional functionality. Kumar and co-workers prepared enzyme-powered organoclay/DNA microcapsules [36] (Fig. 2D). The microcapsules were prepared by electrostatically induced complexation at the surface of DNA and catalase droplets. The buoyancy of the microcapsule was controlled by adjusting the concentration of hydrogen peroxide. And the reversible process of floating and sinking of microcapsule can be controlled by encapsulating magnetic substance into the microcapsule. In addition, Chen's group recently prepared a catalase powered MNM with pH responsive motion behavior by combining catalase with succinylated β -lactoglobulin in porous framework [37]. When $pH > 5$, β -lactoglobulin is permeable, and the fuel will contact with catalase to propel motor. When $pH < 5$, the motor will stop generating bubbles. This work provides good strategy for the responsive control on the motor's movement, as the first reported motor with rapid, reversible pH-responsive motility. The group then studied the directional movement of the motor by controlling the environmental pH [38]. Furthermore, Jang and co-workers attached catalase to protocells, thus prepared a protocellular mimetic of a motile cell [39]. These interesting works can provide more ideas in fabrication and propelling methods for catalase powered EMNMs.

Catalase widely exists in many natural plants. Directly processing specific plants into desired structures can produce EMNMs as well. Wang's group used potato tubers, carrot roots and millet seeds to prepare self-propelled plant-tissue based Janus motor with the size of 2 mm \times 1 mm [40] (Fig. 2E). The directional movement of the motor is achieved by coating one end of the cylinder with inert material to realize

asymmetric structure. Besides, the group prepared a radish tissue-made motor propelled in hydrogen peroxide solution and it could dynamically remove phenolic contaminants from the solution [41]. The direct application of natural materials to yield MNMs is not only cost and time effective, but also environment friendly. Therefore, it is of great significance to directly use natural ingredients to prepare EMNMs. However, the size of the motor is much larger than conventional MNMs. And the integration of extra functions is also challenging, which might limit their future applications.

The high catalytic efficiency of catalase is advantageous to propel motors, but use of toxic fuel of hydrogen peroxide is still an obvious bottleneck problem for its applications. On the one hand, there have been attempts to reduce the required concentration of hydrogen peroxide. On the other hand, scientists are devoting efforts to use other enzyme/fuel combinations to make EMNMs more biocompatible.

2.2.2. Urease powered EMNMs

Although catalase powered EMNMs move fast by bubble propulsion, however, hydrogen peroxide is toxic to living cells and bubbles generated by decomposition of hydrogen peroxide also have adverse effect on organism. On the contrary, urease, the first enzyme discovered by scientists, is widely distributed nature. Its substrate urea is readily available in physiological conditions. Urease can decompose urea into NH_3 (aq) and CO_2 (aq) without generating bubbles. The concentration gradient generated by the decomposition of urea can generate mechanical force for self-propulsion via phoretic mechanism. Therefore, applying urease to power MNMs could greatly improve the biocompatibility of EMNMs.

Ma and co-workers prepared a tubular motor (about 220 nm in diameter) modified with urease [42] (Fig. 3A). They investigated the effect of location of urease and the length of the tube on motor's movement. In addition, the authors synthesized a urease propelled Janus hollow mesoporous silica EMNM [15] (Fig. 3B). The motor can move under physiological concentration of urea. The movement can last more than 10 min and the average speed can reach five body length per second. Besides, the speed of the motor can be controlled artificially. When inhibitor (Ag^+ or Hg^{2+}) is added, the motor would slow down or even stop. Then dithiothreitol (DTT) was continuously added into the solution, urease would regain activation and the motor could resume movement. In addition, by using e-beam deposition to deposit a layer of Fe on the other side of the motor, their movement direction could be controlled by external magnetic field. This work realized the intelligent control of EMNMs' motion behavior and showed great potential in biomedicine.

Sánchez's group then applied urease propelled motor into biomedicine, specifically for drug delivery. They synthesized a urease propelled mesoporous silica-based core shell nanobots, into which doxorubicin (Dox) was loaded. Because of the large surface area of mesoporous silica, the motor has high load capacity [43] (Fig. 3C). And the drug release process can be enhanced by urease triggered movement. Besides, the synergistic effect of drug and ammonia produced by urea is beneficial for killing cancer cells. In addition, the group prepared a urease propelled mesoporous silica motor for controlled drug delivery [44] (Fig. 3D). The outer surface of the motor is grafted with benzimidazole groups and capped by the benzimidazole and cyclodextrin (CD)-modified urease. Even under the presence of urease, loaded drug molecules cannot be released due to the blocking effect of cyclodextrin decorated urease (urease-CD). Only under acidic conditions, drug can be released because of the protonation of benzimidazole and subsequently release of the urease-CD.

Sugai and co-workers recently synthesized a tubular micromotor (1.2 mm outer diameter, 24 mm length) whose inner side was modified with urease by using human serum albumin (HAS) [45] (Fig. 3E). The motor can be hydrolyzed in acidic water (pH 3.0) for 90 min or in a protease mixture (PronaseS) at 37 °C for 120 min, which makes the motor degradable. Such biodegradability through material innovation

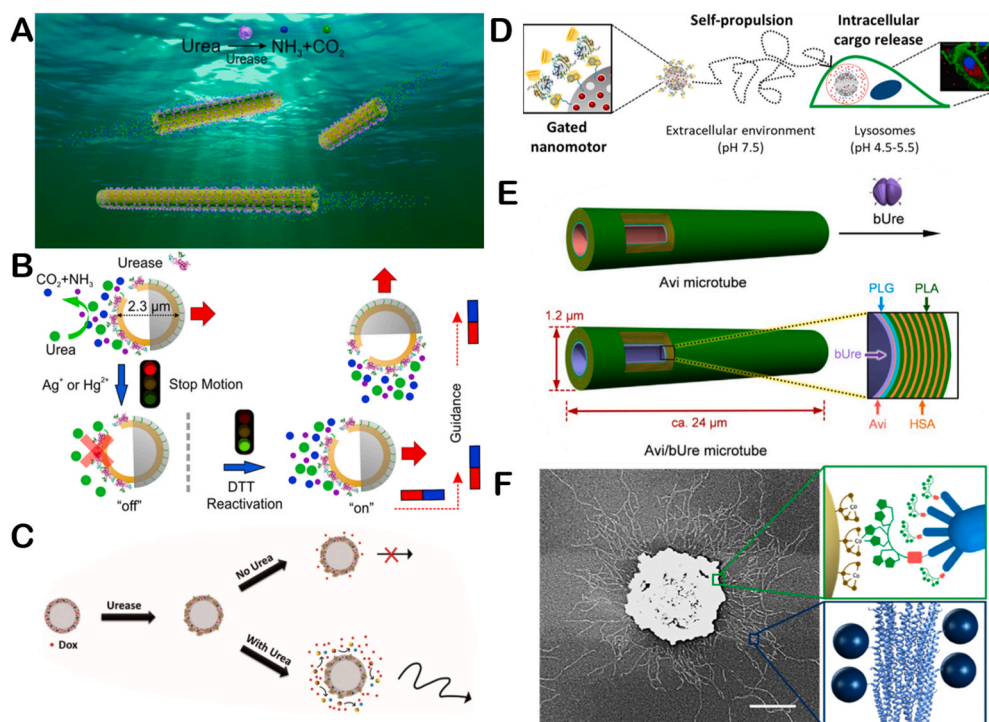


Fig. 3. The illustration of urease powered EMNMs (A) Schematic illustration of urease propelled tubular motor. Reproduced with permission from ref 42. Copyright 2016, American Chemical Society. (B) Schematic illustrating of motion control of urease propelled Janus hollow mesoporous silica EMNM. Reproduced with permission from ref 15. Copyright 2016, American Chemical Society. (C) Schematic illustration of the enhanced drug release of urease propelled nanobots. Reproduced with permission from ref 43. Copyright 2017 Wiley. (D) Schematic illustration of the construction and performance of urease propelled mesoporous silica motor. Reproduced with permission from ref 44. Copyright 2019, American Chemical Society. (E) Preparation of biodegradable urease propelled tubular motor. Reproduced with permission from ref 45. Copyright 2019, Wiley. (F) Schematic illustration of the self-Assembled Phage-Based Colloids applied into micropump. Reproduced with permission from ref 46. Copyright 2019, American Chemical Society.

has improved the biocompatibility of EMNMs. In addition to urease powered EMNMs, scientists have also applied urease to power enzymatic micropumps. Alarcón-Correa and co-workers made micropumps by modifying urease on phage-decorated colloids [46] (Fig. 3F). This approach allows enzymes to maintain high activity, which is also the biocompatible enzyme pump with the fastest fluid flow rate reported to date.

Since the fuels and products from urease powered EMNMs are harmless to lives, they have great biomedical advantages. At present, urease powered EMNMs that can move under physiological concentration of urea have been reported. Scientists have made attempts in applications such as drug delivery and biosensing. The material used to construct the motor is becoming more biocompatible and biodegradable. Therefore, the development of urease powered EMNMs have great

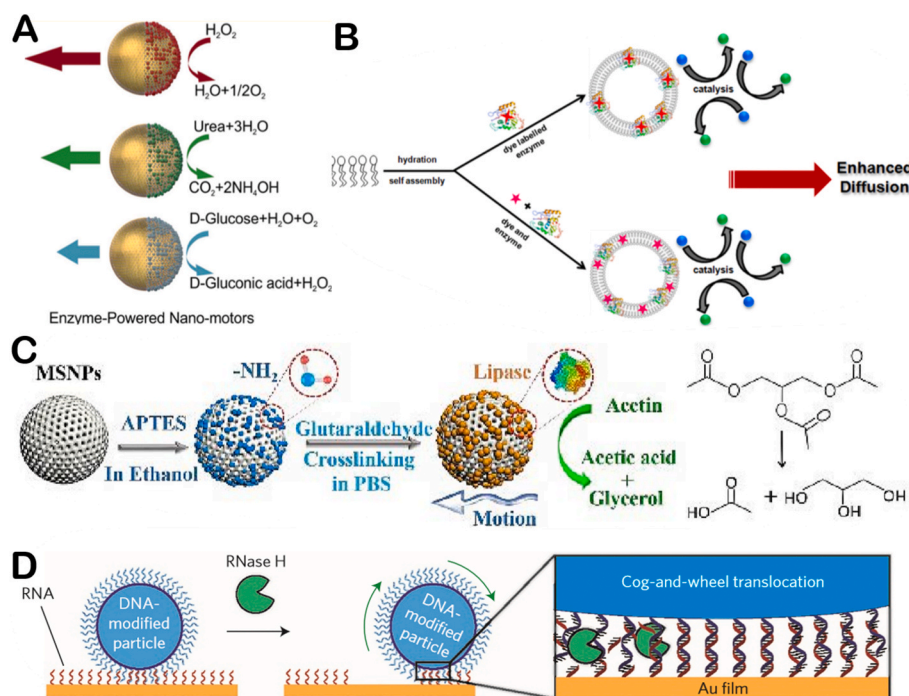


Fig. 4. The illustration of different kinds enzyme powered EMNMs (A) Mesoporous silica spheres based EMNMs half decorated with catalase, urease, and glucose oxidase. Reproduced with permission from ref 47. Copyright 2015, American Chemical Society. (B) Schematic representation showing the enhanced diffusion of enzyme tagged vesicle due to substrate turnover. Reproduced with permission from ref 48. Copyright 2019, American Chemical Society. (C) Schematic representation of the functionalization strategy for the preparation of the lipase-based nanomotors. Reproduced with permission from ref 50. Copyright 2019, Wiley. (D) Schematic representation of the movement mechanism of DNA-modified particles. Reproduced with permission from ref 52. Copyright 2016, Nature.

potential in future motors' assisted nanomedicine.

2.2.3. Other enzymes powered EMNMs

Applying different kinds of enzymes to EMNMs not only can increase their diversity, but also realize different functions of motors. Ma and co-workers chemically linked three enzymes (catalase, urease, glucose oxidase) to the surface of mesoporous silica spheres [47] (Fig. 4A). All three motors can move in the presence of fuel. They systematically studied the motors' motion characteristics. Sen's group used two biocompatible substances, which are ATPase and phospholipid vesicles, to synthesize an EMNM [48] (Fig. 4B). ATPase is attached to the membrane surface of the phospholipid vesicles. They proved that the presence of ATP would increase the diffusion of the motor. And the group also studied the fluid transport mechanism of phosphatase micropumps which is determined by the density difference of reactants and products [49]. Finally, they proved that exothermic reaction has little effect on acceleration of fluid flow. Wang and co-workers prepared a lipase-driven mesoporous silica motor by decomposition of triethyl acetate [50] (Fig. 4C). The motor's enhanced diffusion can last for 40 min. It can actively clean melamine oil droplets with high degradation efficiency. Bath and co-workers prepared a linear motor which is built by DNA and restriction enzyme [51]. The motor can move DNA cargo in discrete steps along DNA tracks which is powered by nicking enzyme that cuts tracks. Damage of tracks makes the motor move directionally. But the speed of the motor is very low at 0.1 nm/s. After that, Yehl and co-workers prepared a ball motor with rolling motion driven by RNase H [52] (Fig. 4D). DNA-based walkers could typically move at very low speed (~1 nm/s), but the ball motor moves three orders of magnitude faster than traditional walkers. The motor is a DNA-modified spherical particle that hybridize to RNA-modified surfaces. By adding RNase H, the motor could move due to the selective hydrolysis so that the motor could be self-guided. This work provides new idea for the development of DNA-based walkers.

2.3. Multiple enzymatic reactions propelled EMNMs

Although catalase powered EMNMs move fast, their fuel hydrogen peroxide is biotoxic. Besides, some EMNMs have the disadvantage of low speed. To solve such problems, multiple enzymatic reactions propelled EMNMs have been developed. Besides, applying different enzymes to EMNMs can not only propel motors, but also enable motors to achieve more functions. Using more kinds of enzymes can diversify motors' movement environment and expand the application range of EMNMs.

With the hope of solving the toxicity problem of H_2O_2 fuel, researchers prepared cascade enzymatic reactions propelled EMNMs by simultaneously loading glucose oxidase (GOx) and catalase on EMNMs, in which case glucose will first be decomposed into H_2O_2 , which then is decomposed by catalase to generate driving force. In this way, the biological toxicity of hydrogen peroxide problem is well solved. Besides, loading multiple enzymes on one motor will combine multiple propelling systems on one motor to improve its speed. Multiple enzymatic reactions can enrich the application scenarios of EMNMs and improve their moving efficiency.

Early, Mano and co-workers used carbon fiber modified with the two enzymes to prepare a motor [53] (Fig. 5A). One end of the fiber is modified with GOx and redox polymer I, while the other end is bilirubin oxidase (BOD) and redox polymer II. Electrons would transfer from the GOx side to the BOD side and generate O_2 when the motor contacted with buffer solution with pH = 7 containing 10 mM glucose. The motor is propelled by electron flow between solution and O_2 . When insulator exists in the middle of the two sides, the motor could not move. The motor is propelled by bioelectrochemical action of the two enzymes. This work pioneered the use of multiple enzymes to power EMNMs. Similarly, Pavel and co-workers prepared a kind of nanorod whose motion is enhanced through biocatalytically induced self-electrophoresis [54].

Attaching GOx and catalase on EMNMs simultaneously is a great

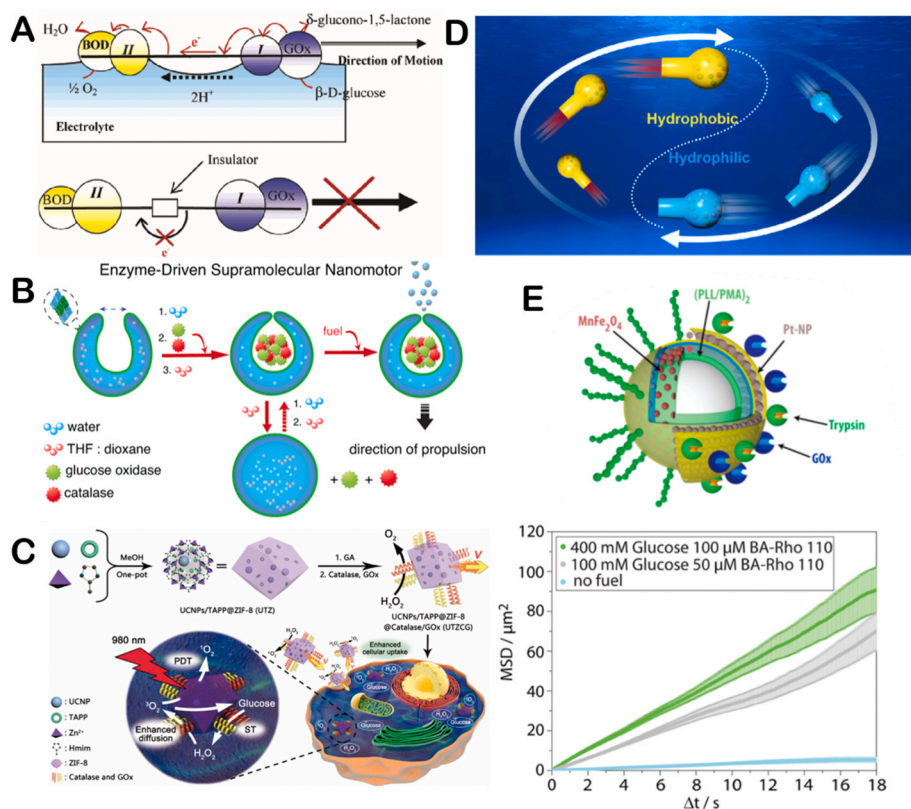





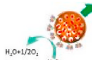
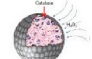
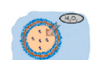


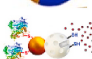
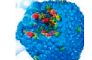


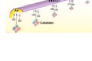
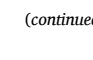






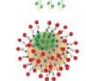

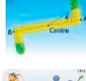
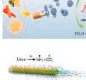
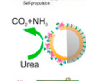
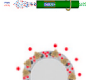
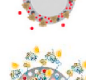



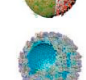
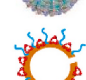


Fig. 5. The illustration of multiple enzymatic reactions propelled EMNMs (A) Schematic representation of the component and motion mechanism of carbon fiber. Reproduced with permission from ref 53. Copyright 2005, American Chemical Society. (B) Schematic representation of enzyme-loaded supramolecular nanomotor. Reproduced with permission from ref 57. Copyright 2016, American Chemical Society. (C) Schematic illustration of the fabrication and synergetic photodynamic-starvation therapy process of UTZCG nanomotor. Reproduced with permission from ref 59. Copyright 2019, Elsevier. (D) Schematic illustration of carbonaceous nanoflask (CNF) motors. Reproduced with permission from ref 60. Copyright 2019, American Chemical Society. (E) Schematic representation of the motor consisting of glucose oxidase (GOx)-Pt and trypsin and its MSD analysis under different fuel concentrations. Reproduced with permission from ref 61. Copyright 2017, American Chemical Society.

Table 1
The classification and introduction of EMNMs.

Types of EMNMs		Movement mechanism	Materials	Fuel	Motion environment	Motion speed	Application	Schematic diagram	Ref
Single enzymatic reaction propelled EMNMs	Catalase	Molecule motors and enzymes as motors	Synthesis and decomposition of ATP	Myosin, dynein and kinesin	ATP	–	–		16,17,18
		Synthesis and decomposition of ATP	ATP synthase	ATP	–	–	–		20
		Enzyme-enhanced diffusion	Urease	Urea	Water	–	–		24
		Enzyme-enhanced diffusion	DNA polymerase	Nucleotide	Buffer solution	–	Micro/nanopump		26
		Bubbles propulsion	Ti/Au film	H ₂ O ₂	Water	226.1 ± 21.1 μm/s in 1.5% H ₂ O ₂	–		28
		Bubbles propulsion	Fpoly(ethylene glycol) diacrylate and dextran	H ₂ O ₂	Water	102.96 ± 2.08 μm/s in 4% H ₂ O ₂	–		32
		Bubbles propulsion	Mesoporous silica	H ₂ O ₂	Water	–	Drug delivery		34
		Bubbles propulsion	Organoclay/DNA semipermeable microcapsules	H ₂ O ₂	Water	–	Motor functionalization		36
		Bubbles propulsion	Biotinylated polymer vesicles	H ₂ O ₂	Water	–	Biomedical application		39
		Bubbles propulsion	Bovine serum albumin/poly- l-lysine (PLL/BSA) multilayer	H ₂ O ₂	PBS solution	68 μm/s in 0.5% H ₂ O ₂	Drug delivery		112
		Bubbles propulsion	Polymer capsules	H ₂ O ₂	–	232 μm/s in 2% H ₂ O ₂	Drug delivery		96
		Bubbles propulsion	Janus Au–mesoporous silica	H ₂ O ₂	PBS solution	–	Drug delivery		113
		Bubbles propulsion	Metal–organic frameworks	H ₂ O ₂	–	–	Drug delivery		37
		Bubbles propulsion	Polymersomes	H ₂ O ₂	–	–	Drug delivery		33
		Bubbles propulsion	Polymer based bottlebrush	H ₂ O ₂	a viscous tumor microenvironment gel model	–	Overcoming tissue penetration barrier		35
		Bubbles propulsion	PEDOT/Au bilayer microtubes	H ₂ O ₂	Water	54.0 ± 3.5 μm/s in 2% H ₂ O ₂	Biochemical sensing		29
Bubbles propulsion	PEDOT/Au bilayer microtubes	H ₂ O ₂	Water	380 μm/s in 2% H ₂ O ₂	Biochemical sensing		120		


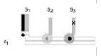

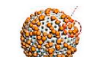

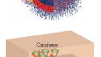

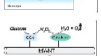

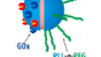




(continued on next page)

Table 1 (continued)

Types of EMNMs	Movement mechanism	Materials	Fuel	Motion environment	Motion speed	Application	Schematic diagram	Ref
Urease	Bubbles propulsion	PEDOT/Au microtubes	H ₂ O ₂	Water	411 ± 40 μm/s in 5% H ₂ O ₂	Biochemical sensing		124
	Bubbles propulsion	PEDOT-PSS/Au microtubes	H ₂ O ₂	Water	~51 μm/s in 0.25% H ₂ O ₂	Biochemical sensing		30
	Bubbles propulsion	Multi-metallic (Au/Ag/Ni/Au)	H ₂ O ₂	Water	~209 μm/s in 1.5% H ₂ O ₂	Biochemical sensing		95
	Bubbles propulsion	Iron oxide particles	H ₂ O ₂	Water	–	Biochemical sensing		125
	Bubbles propulsion	PSMA/PS mixtures	H ₂ O ₂	PBS solution	19–69 μm/s in 3.5% H ₂ O ₂	Biochemical sensing		127
	Bubbles propulsion	Silk fibroin	H ₂ O ₂	–	–	Microstirrers		131
	Bubbles propulsion	Plant tissues	H ₂ O ₂	Water	–	Environmental remediation		41
	Phoretic propulsion	Silica	Urea	Water	~5.25 μm/s in 0.1 mol/L urea	Biomedical application		42
	Phoretic propulsion	Mesoporous silica	Urea	Water	~8 μm/s in 0.05 mol/L urea	Drug delivery		15
	Phoretic propulsion	Protein	Urea	PB solution	2.7 ± 0.2 μm/s in 0.1 mol/L urea	Biomedical application		45
	Phoretic propulsion	Mesoporous silica	Urea	Water and ionic media	–	Drug delivery		43
	Phoretic propulsion	Mesoporous silica	Urea	Water and PBS	–	Drug delivery		44
	Phoretic propulsion	Mesoporous silica	Urea	Urine	–	Targeted bladder cancer therapy		117
	Phoretic propulsion	Platelet cell	Urea	PBS solution	–	Drug delivery		118
	Phoretic propulsion	Mesoporous silica	Urea	Ficoll solutions	–	Drug delivery		119
	Phoretic propulsion	Mesoporous SiO ₂	Urea	Water	6.49 μm/s in 0.05 mol/L urea solution	Photodynamic therapy		90
	Phoretic propulsion	Mesoporous silica	Urea	PBS solution	–	Biochemical sensing		126

(continued on next page)

Table 1 (continued)

Types of EMNMs		Movement mechanism	Materials	Fuel	Motion environment	Motion speed	Application	Schematic diagram	Ref
Other enzymes	ATPase	Phoretic propulsion	Phospholipid vesicles	ATP	Buffer solution	–	–		48
	Nicking enzyme	Nicking enzyme that cuts tracks	DNA and restriction enzyme	–	–	0.1 nm/s	–		51
Multiple enzymes	RNase H	Hydrolysis of hybridized RNA	DNA and RNA	RNase H	–	–	–		52
	Lipase	–	Mesoporous silica	triacetin	PBS solution	–	Environmental remediation		50
	GOx-Cat	Bubbles propulsion	Asymmetric polymersome	Glucose	–	–	Drug delivery		116
	Catalase, urease, lipase, GOx	–	–	H ₂ O ₂ , Urea, Glucose	–	–	Micropumps		128
	GOx bilirubin oxidase	Electrophoresis	Carbon fiber	Glucose	Buffer solution	~1 cm/s in 0.01 mol/L glucose	–		53
	GOx and catalase	Bubbles propulsion	Carbon nanotubes	Glucose	Water	–	–		55
	GOx and catalase	Bubbles propulsion	Colloids	Glucose	Buffer solution	–	Drug delivery		56
	GOx and catalase	Bubbles propulsion	Polymer	Glucose	–	~11 μm/s in 0.01 mol/L glucose	Drug delivery		57
	GOx and catalase	Bubbles propulsion	Polymer	Glucose	–	–	–		58
	GOx and catalase	Bubbles propulsion	Metal–organic frameworks	Glucose	–	–	Photodynamic therapy		59
	GOx and catalase	Bubbles propulsion	Carbonization of L-CNF	Glucose	Water	~0.4 μm/s in 0.01 mol/L glucose	–		60
	GOx and trypsin	Bubbles propulsion and phoretic propulsion	Inorganic substance	Glucose, BA-Rho-110	Water	0.72 μm/s in 0.4 mol/L glucose and 0.1 μmol/L BA-Rho-110 solution	–		61

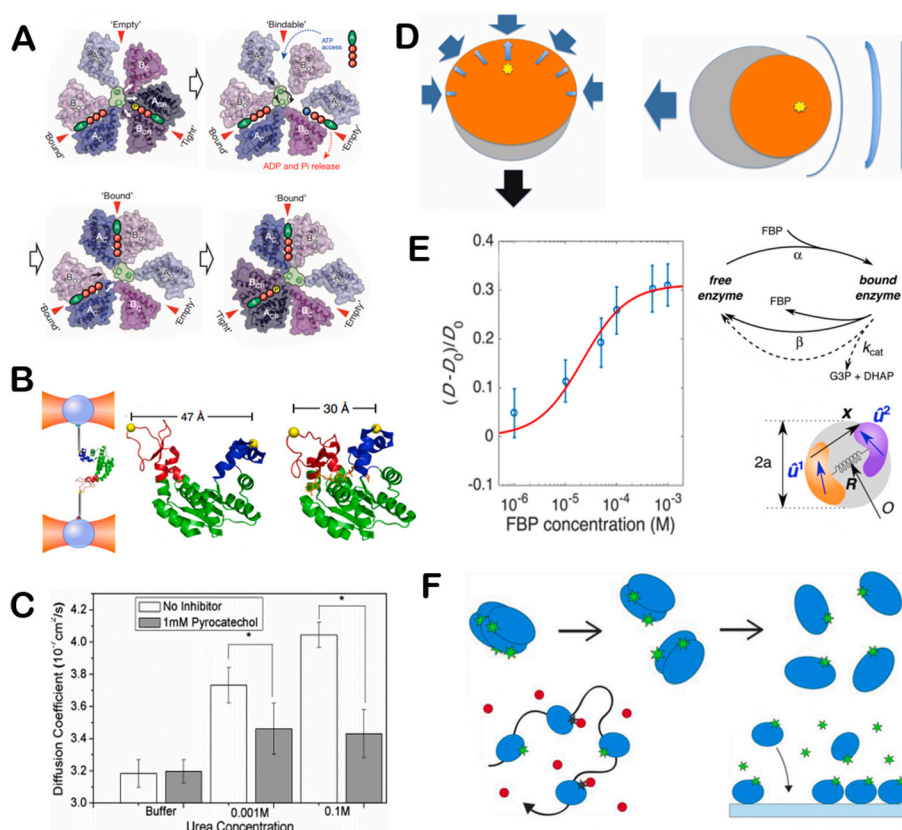


Fig. 6. Study on the propulsion mechanism of single enzyme. (A) The model of the rotation mechanism of V₁-ATPase. Reproduced with permission from ref 73. Copyright 2013, Nature. (B) Measurement of single molecular force with optical tweezers and the structure of the open and closed conformation of Adk. Reproduced with permission from ref 75. Copyright 2016, Nature. (C) The diffusion coefficient of urease increased with the increase of concentration. Reproduced with permission from ref 80. Copyright 2010, American Chemical Society. (D) Schematic representation of the center of protein mass translation and drive the motion of enzyme due to chemoacoustic effect. Reproduced with permission from ref 79. Copyright 2014, Nature. (E) The diffusion coefficient of aldolase in the presence of substrate, the structural model of aldolase and two stochastic state for free enzyme and bound enzyme. Reproduced with permission from ref 81. Copyright 2017, American Chemical Society. (F) The enhancement diffusion of enzyme in the process of FSC measurement may be caused by the dissociation of enzyme, the combination of surface and glass or the substrate-induced fluorescence quenching. Reproduced with permission from ref 82. Copyright 2018, American Chemical Society.

attempt and successfully resolve the toxicity of hydrogen peroxide problem. Early, Pantarotto and co-workers attached the two enzymes on carbon nanotubes and successfully realized the propulsion of carbon nanotubes [55]. Later, Schattling and co-workers studied the enhanced

diffusion of sub-micron-sized Janus particles modified with the two enzymes in the presence of glucose [56]. Then, Abdelmohsen and co-workers assembled GOx and catalase into a bowl-shaped polymer to realize the movement of the motor in glucose solution at physiological

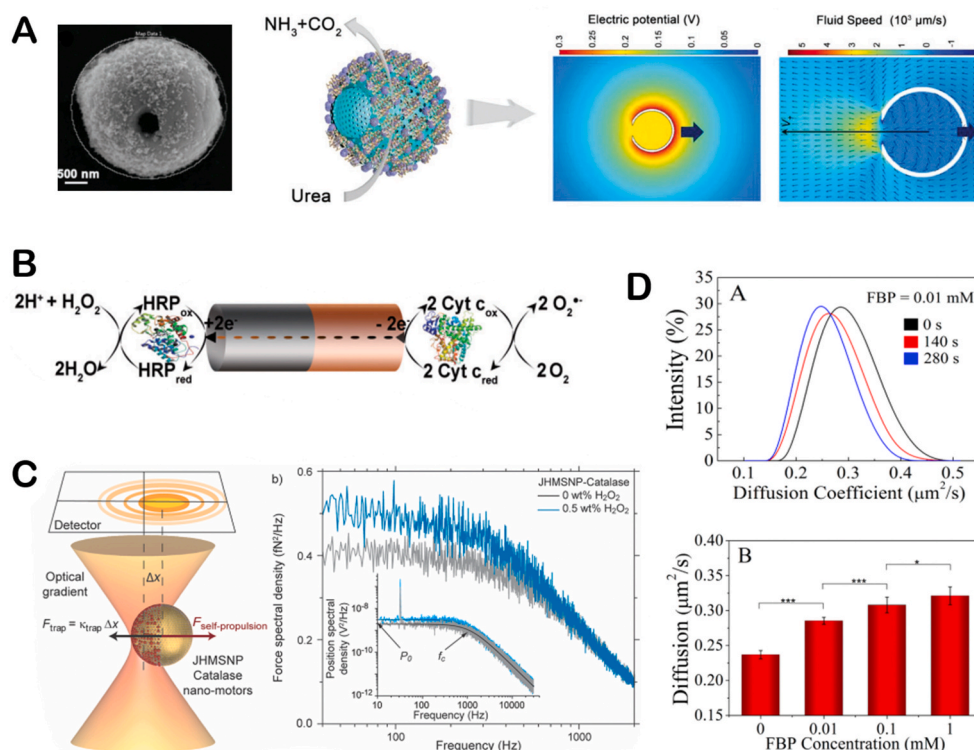


Fig. 7. Propulsion mechanisms of synthetic EMNMs. (A) The structure of the MHSTU, and the formation of electric field and electron flow. Reproduced with permission from ref 90. Copyright 2019, Wiley. (B) The bio-electrochemical mechanism of propulsive PPy-Au nanorod in O₂ and H₂O₂ solutions. reproduced with permission from ref 54. Copyright 2014, Wiley. (C) The schematic illustration of measuring the force produced by JHMSNP-catalase nanomotors. Reproduced with permission from ref 47. Copyright 2015, American Chemical Society. (D) The diffusion coefficient of aldolase in endothermic reaction with different time and concentration. Reproduced with permission from ref 93. Copyright 2017, American Chemical Society.

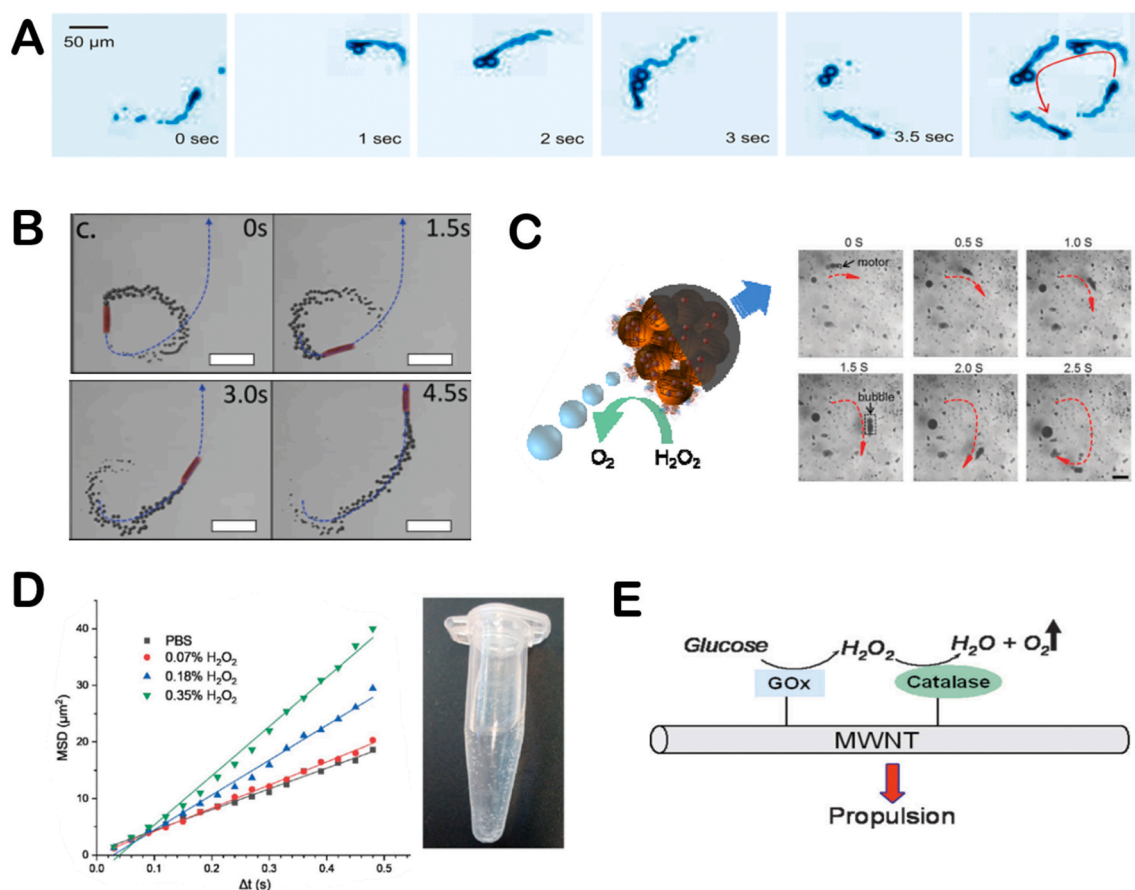


Fig. 8. The bubble propulsion mechanisms of EMNMs. (A) The motion of the hybrid microengine was powered by the generation of “front-side bubbles”. Reproduced with permission from ref 28. Copyright 2010, American Chemical Society. (B) The trajectory of the catalase-modified microrocket in 0.1 wt% H_2O_2 solution. Reproduced with permission from ref 94. Copyright 2016, Wiley. (C) The schematic illustration of propulsion of the bio-catalytic Janus motor and a video clip of the motor’s trajectory. Reproduced with permission from ref 97. Copyright 2014, Royal Society of Chemistry. (D) The change of MSD values and the formation of oxygen bubbles with the addition of H_2O_2 . Reproduced with permission from ref 14. Copyright 2018, Royal Society of Chemistry. (E) The propulsion mechanism of MWCNTs decorated with GOx and catalase. Reproduced with permission from ref 55. Copyright 2008, Royal Society of Chemistry.

concentration [57] (Fig. 5B). Due to the protection of the polymer, the encased enzymes would not be hydrolyzed by proteases. After that, Toebes and co-workers prepared a biodegradable bowl-shaped motor by functionalizing the motor surface with GOx and catalase [58]. This work improves the biocompatibility of motors. Recently, You and co-workers applied GOx and catalase powered motor to achieve synergistic therapeutic effect of photodynamic therapy (PDT) and starvation therapy (ST) [59] (Fig. 5C). GOx can digest glucose in cells and starve the cells. The hydrogen peroxide generated in the former process can not only propel motors but also generate singlet oxygen to promote PDT. Thus, the two enzymatic cascade reactions form a positive feedback for the whole therapeutic system, which greatly improve the efficiency of PDT and ST. In addition, Gao and co-workers applied the system to carbonaceous nanoflask (CNF) motors, and studied the influence of the hydrophilicity and hydrophobicity of the motor on its movement behavior [60] (Fig. 5D). Thus, the synergistic effect of GOx and catalase is beneficial to the biomedicine use of EMNMs.

The GOx/catalase system utilizes one reaction product serving as the fuel of another reaction to propel motors. However, multiple enzymatic reactions taking place simultaneously on the same motor can increase the motor’s speed. Schattling and co-workers separately prepared two motors modified with glucose oxidase (GOx)-Pt and trypsin which can be propelled at the present of glucose and peptides [61]. They studied the two motors’ movement. Then a dual enzyme propelled motor was prepared by combining two catalytic systems on the same motor

(Fig. 5E). They found that in the present of two fuels, the motor’s speed was enhanced. This research provides a method to improve the speed of EMNMs by using multiple enzyme/fuel combinations.

Through the above paragraph we introduced many kinds of EMNMs, including: molecular motors, single enzyme motors, catalase powered EMNMs, urease powered EMNMs, and other single enzyme powered EMNMs. And we also introduced multiple enzymatic reactions propelled EMNMs. We summarized these motors’ movement mechanism, materials, applications in Table 1 as following.

3. Fundamental propulsion mechanism of enzymatic motors

At micro/nano-scale, the movement of small objects in low Reynolds number fluid need to overcome the inherent Brownian motion, the viscous force of solution [62]. Therefore, the self-propulsion mechanism of the micro/nanomotors is complicated and influenced by many factors, like the origins of driving force, motor size and shape. Some of the physics such as Reynolds number, flow regimes behind the motion behavior of the motors, as well as corresponding tracking and analyzing techniques and skills about the self-propulsion of motors have been well addressed in previous literature [7,62,63]. In this section, we review up-to-date fundamental knowledge about fundamental propulsion mechanisms underlying the movement of single enzyme and enzymes propelled structures.

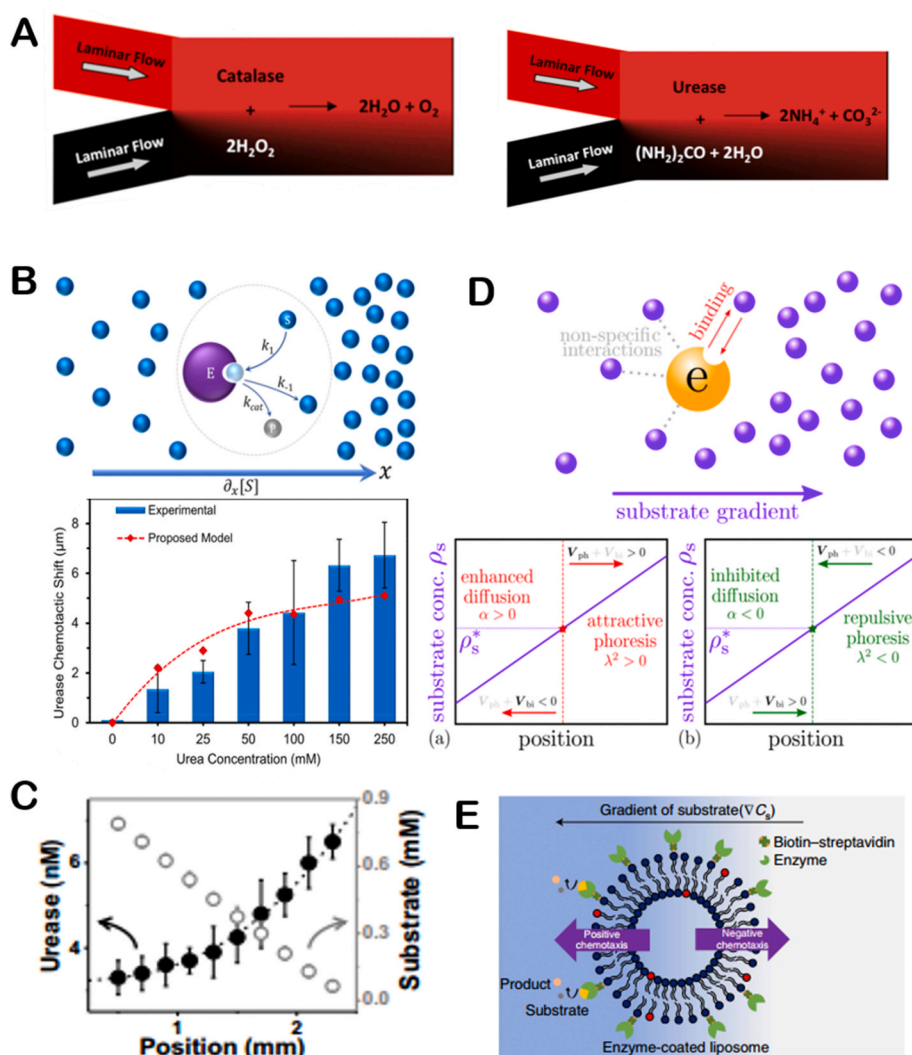


Fig. 9. The chemotaxis of EMNMs. (A) Chemotaxis of catalase and urease. Reproduced with permission from ref 25. Copyright 2013, American Chemical Society. (B) Schematic diagram of enzyme in concentration gradients of substrates, and the experimental and theoretical results of urease chemotaxis. Reproduced with permission from ref 103. Copyright 2018, American Chemical Society. (C) Anti-chemotaxis of urease catalyzing urea hydrolysis in a microfluidic channel. Reproduced with permission from ref 105. Copyright 2018, PNAS. (D) Competition between the phoresis and binding-induced diffusion changes at different substrate concentrations. Reproduced with permission from ref 87. Copyright 2018, American Chemical Society. (E) The positive or negative migration of enzyme-coated liposomes on the basis of enzymatic propulsion or solute interactions. Reproduced with permission from ref 106. Copyright 2019, Nature.

3.1. Mechanism of propulsion force by single enzyme

For the motion of single enzyme, researchers proposed that the conformational transition play an important role for the force generation during enzymatic reaction [64–69]. For instance, it has been found that the rotational movement of ATPase is achieved through conformational change of enzyme. The F- and V-ATPases, are important motor complexes anchored to organelle membranes and participate in the hydrolysis or synthesis of ATP during the proton transport [70]. In 1979, Boyer predicted the rotational mechanism of F-ATPase firstly. Until now, many studies have demonstrated the rotational catalysis of ATPases, and it is widely accepted that the rotation of ATPases was induced by the conformational transition of subunits [71,72]. Arai and co-workers provided a high resolution view of the V_1 -ATPase rotation that showed conformational change due to nucleotide binding, and suggested the right-handed binding order with a cooperative manner [73] (Fig. 6A). Not only the motion of single enzyme *in vivo*, but the diffusion movement of various free-enzymes *in vitro* has been reported in recent years [74], which is also found to be closely related to the conformational change of enzymes. Pelz and co-workers used single-molecule force spectroscopy to measure the substrate dependence forces that drives the Adenylate kinase (AdK) to form a closed conformation, which helped us to further understand the energy-driven forces produced by conformational changes of enzymes due to substrate binding [75] (Fig. 6B). In addition, scientists proposed that the

conformational transition would lead to hydrodynamic interactions in solution. Considering the conformational cycles of molecular machines and hydrodynamic effect, T. Sakaue and co-workers constructed a model to obtain the analytical estimates for the propulsion velocity and the stall force [76,77]. Therefore, the enhancement of enzyme diffusion may be due to conformational fluctuations arising from the substrate binding or unbinding in the presence of their substrates.

It has been demonstrated that the motion of enzymes can be achieved by converting chemical energy into mechanical forces through a catalytic reaction, and the phenomenon of enhanced diffusion of enzymes can be observed. But at present, the possible mechanism behind the biocatalytically induced enhanced diffusion of enzymes is still controversial. Apart from the conformational transition of enzymes, the phoresis [13,78] and thermal effects [79] were proposed to explain the experimental phenomenon. Muddana and co-workers for the first time reported the single-molecule scale measurement of urease-catalyzed enhanced diffusion (Fig. 6C). This work showed that the enzyme exhibited enhanced diffusion in the presence of concentration gradients of specific substrate, and they discussed the mechanism by which urease enhances diffusion should be self-diffusiophoresis mechanism [25,80]. Riedel and co-workers proposed that the relationship between enhanced diffusion and thermal effect during catalytic reaction [79]. The authors analyzed the single-molecule fluorescence correlation spectra data within a random theoretical framework, and proposed the chemoacoustic effect. It explained that the release of heat during the catalytic

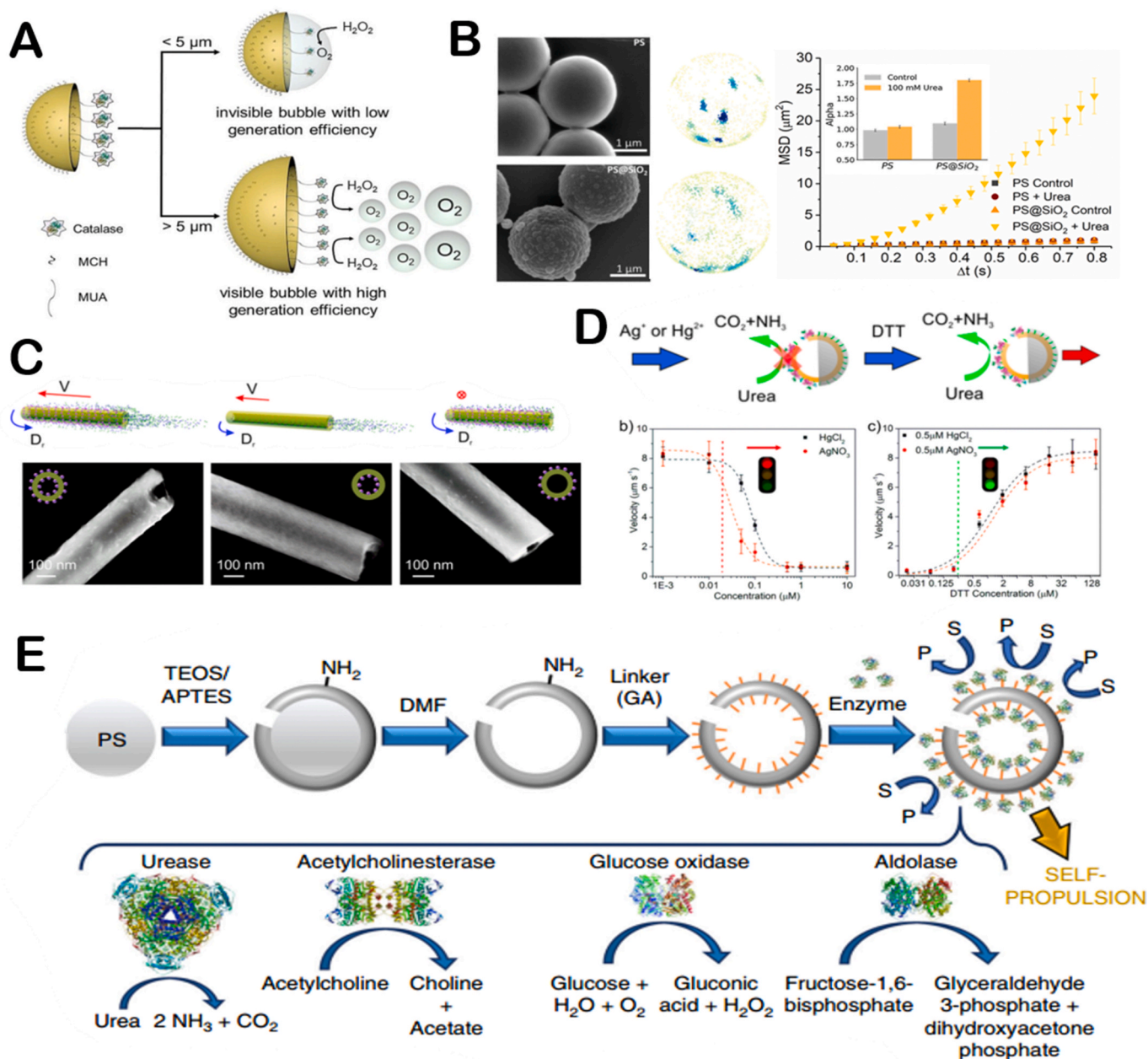


Fig. 10. The affecting factors of EMNMs. (A) The effect of the size of microshell motors on the motion mechanism, reproduced with permission from ref 107. Copyright 2019, Wiley. (B) The SEM micrographs and 3D density maps of PS- and PS@SiO₂ based motors, comparison of MSD and velocity of PS and PS@SiO₂ micromotor in the presence or absence of fuel. Reproduced with permission from ref 109. Copyright 2018, American Chemical Society. (C) The different urease distribution on the nanotubes and the corresponding SEM micrograph. Reproduced with permission from ref 42. Copyright 2016, American Chemical Society. (D) The motion control of EMNMs by inhibiting or reactivating enzyme activity. Reproduced with permission from ref 15. Copyright 2016, American Chemical Society. (E) Schematic diagram of fabrication of self-propelled EMNMs functionalized with different kinds of enzymes. Reproduced with permission from ref 111. Copyright 2019, Nature.

reaction produces an asymmetric pressure wave, which results in an interfacial stress between the protein and the solvent, and the center of mass of the enzyme is temporarily replaced (Fig. 6D). And then Golestanian discussed and examined four mechanisms that could lead to diffusion enhancement of active enzymes, including boost in kinetic energy, self-thermophoresis, stochastic swimming and collective heating [69]. In this work, it is concluded that the last two mechanisms can reasonably account for the experimental results of effective diffusion. And they suggested the diffusion enhancement of the enzyme in the exothermic reaction may be contributed to a combination of the increase

of the global temperature in the sample container and the enhancement of the conformational change that result in the hydrodynamic enhancement of effective diffusion coefficient. Two years later, however, Sen and Golestanian's group employed a relatively slow adolase that catalyzes an endothermic reaction, which also exhibited the enhanced diffusion induced by substrate [81] (Fig. 6E). The experimental results showed that the exothermic property of the catalytic reaction was not a necessary condition for enhanced diffusion.

Generally, fluorescence correlation spectroscopy (FCS) and dynamic light scattering (DLS) are used to measure the enhanced diffusion

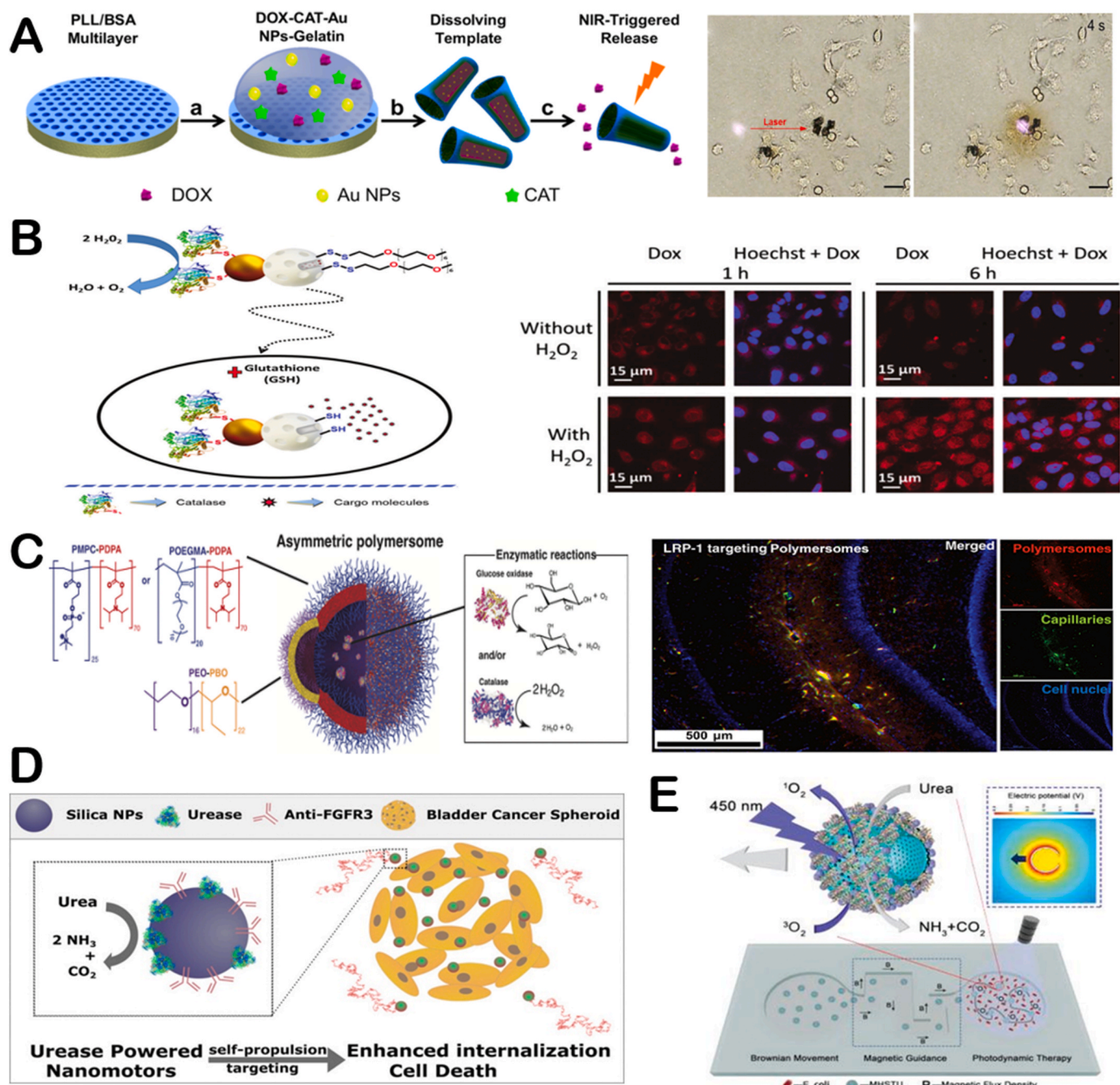


Fig. 11. Biomedical applications of EMNMs. (A) The transportation and light responsive release of drug by protein-based microrockets. Reproduced with permission from ref 112. Copyright 2014, American Chemical Society. (B) The self-propulsion of nanobots and glutathione-responsive cargo delivery, confocal microscopy images of HeLa cells treated with nanobots in the absence and presence of H_2O_2 . Reproduced with permission from ref 113. Copyright 2019, Royal Society of Chemistry. (C) Schematic illustration of asymmetric polymersomes, immunofluorescence histology of rat hippocampus sections treated with asymmetric polymersomes loaded with GOx + Cat. Reproduced with permission from ref 116. Copyright 2017, Science. (D) Targeting 3D bladder cancer spheroids by urease biocatalytic nanomotors. Reproduced with permission from ref 117. Copyright 2019, American Chemical Society. (E) The mobile photosensitizer platform for antibacterial photodynamic therapy based on urease-powered micromotors. Reproduced with permission from ref 90. Copyright 2019, Wiley.

behavior of enzymes. The FCS experiments have shown that the diffusion coefficient of some enzymes increased when the enzyme have catalytic activity [25,80]. However, a new phenomenon has recently been discovered by Fischer's group to explain the enhanced diffusion behavior of enzymes. It is demonstrated that the diffusion coefficient of enzymes significantly altered, which may be due to the artifacts such as the dissociation of enzyme and surface binding to glass or substrate-induced fluorescence quenching during FCS measurements [82] (Fig. 6F). Besides, the same group measured the absolute diffusion

coefficient of aldolase using Pulsed Field Gradient Nuclear Magnetic Resonance (PFG-NMR), and found that the active aldolase did not exhibit any enhanced diffusion behavior [83]. This is consistent with the results reported by Hess's group who utilized the DLS to measure the diffusion coefficient of aldolase in the presence or absence of its substrates [84]. These findings contradict the results from FCS experiments previously reported. And others have shown that some oligomeric enzymes dissociate into subunits at substrate concentration above K_M , which are diffused more rapidly. It provided a simple mechanism to help

explain the enhanced diffusion behavior in this concentration range [85]. But these arguments are still controversially, Xu and co-workers studied the oligomerization state of enzymes with the single-molecule imaging. And their results suggested that it can rule out the possibility that diffusion enhancement is induced by dissociation of enzyme [86].

3.2. Propulsion mechanism of EMNMs

Inspired by the natural molecular motors in living organisms, a series of artificial EMNMs have been reported, which are composed of different kinds of enzymes and types of micro/nano-structures (such as materials, shapes, sizes, etc.) [62]. Many studies have shown that enzymes can act as engines to drive larger synthetic structures through different propulsion mechanisms.

3.2.1. Phoretic mechanism

The small objects can swim in the fields or gradients generated around them through phoretic mechanisms, which means that the gradient of the field, including electrostatic potential, temperature and concentration, can drive the motion of the objects [78]. From a theoretical perspective, it has proposed the self-phoretic effects (electrophoresis, thermophoresis, diffusiophoresis) would drive the motion of molecular machines [78,87,88]. The experimental phenomena supported this view and proved that the phoretic mechanism of some motion systems was essential. Earlier, the self-propelled bioelectrochemical motor was reported by Mano and Heller [53]. They designed a carbon

fiber decorated with GOx and bilirubin oxidase (BOD) at each end that moved by bioelectrochemical propulsion at the water-O₂ interface. When the redox occurred on the nanorods, the fiber was propelled through the electron flow at the solution-O₂ interface. And then, Gaspar's group decorated each end of the polypyrrole-gold (PPy-Au) nanorod with different heme proteins [54,89]. It is found that the diffusion motion of the nanorods increased with the concentration of hydrogen peroxide. They explained that the motion behavior was produced by self-electrophoresis of the nanorods. The electrons transferred from one end to the other because of oxidation or reduction reactions at the ends of the nanorods, driving the nanorods to move in opposite directions (Fig. 7B). Except for the self-electrophoresis mechanism, the urease-propelled motors have been reported that the directional self-propulsion driven by a self-diffusiophoresis mechanism [15]. Ma's group further explained, based on a qualitative and simplified model, that the urease-powered magnetic hollow mSiO₂ motors (MHSTU) was driven by an ionic diffusiophoresis mechanism [90]. It was pointed that the diffusing rate of OH⁻ and NH₄⁺ ions are different in solution would spontaneously form an electric field, and because of the inherent asymmetric property of the MHSTU (a hole in hollow mSiO₂), the electric field would be deformed and the electro-osmotic flow would be induced to point toward the hole (Fig. 7A). Recently, the assumptions about Debye length and weak non-equilibrium effects in the classical phoretic models were relaxed by Corato and co-workers, and the self-propulsion process of charged colloidal particles releasing ions was studied [91]. In the model, the ions released by the particles throw the system off

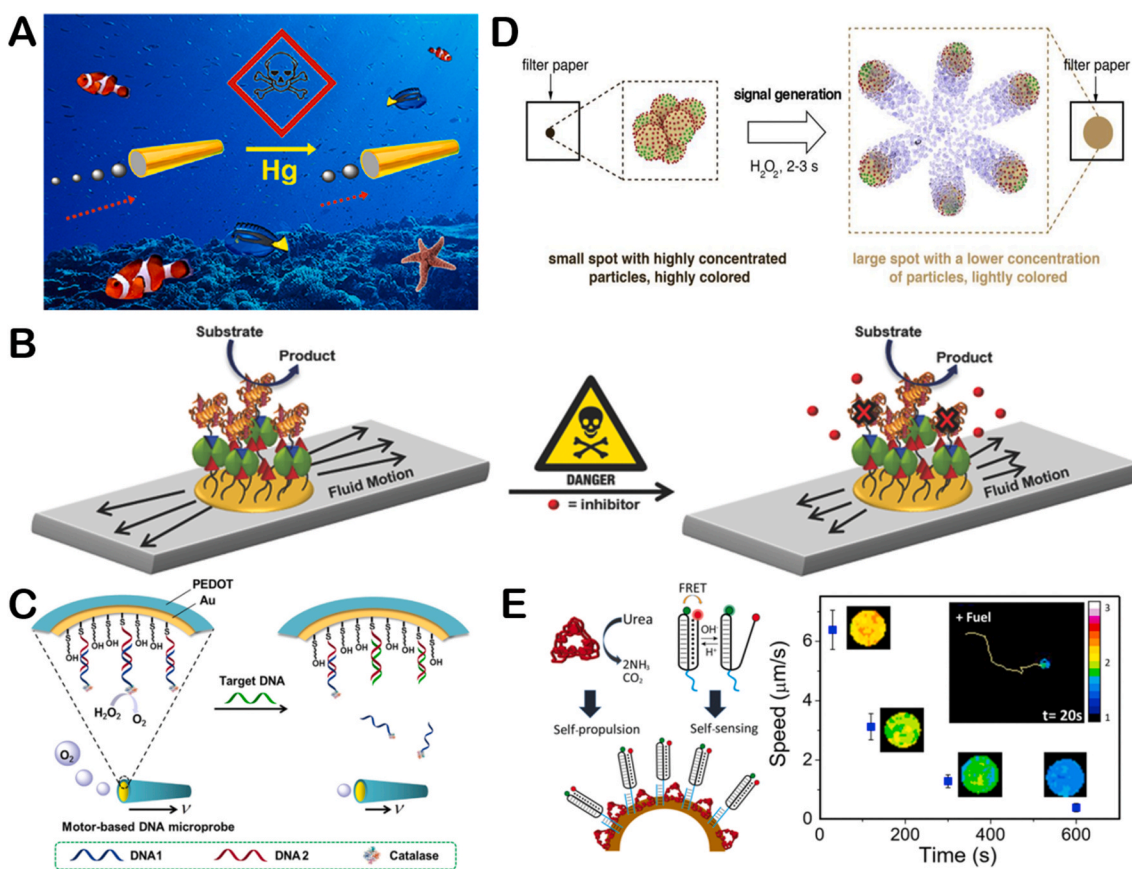


Fig. 12. The biochemical sensing using EMNMs. (A) Water quality testing by catalase powered microfish. Reproduced with permission from ref 29. Copyright 2013, American Chemical Society. (B) Detection of inhibitor by enzyme powered pumps. Reproduced with permission from ref 121. Copyright 2016, Wiley. (C) Catalase powered micromotors for target DNA detection. Reproduced with permission from ref 124. Copyright 2017, Elsevier. (D) Multifunctional Janus particles for colorimetric detection of sepsis biomarkers. Reproduced with permission from ref 125. Copyright 2019, Elsevier. (E) The monitoring of pH change and micromotors intrinsic activity by urease-powered micromotors modified with DNA nanoswitch. Reproduced with permission from ref 126. Copyright 2019, American Chemical Society.

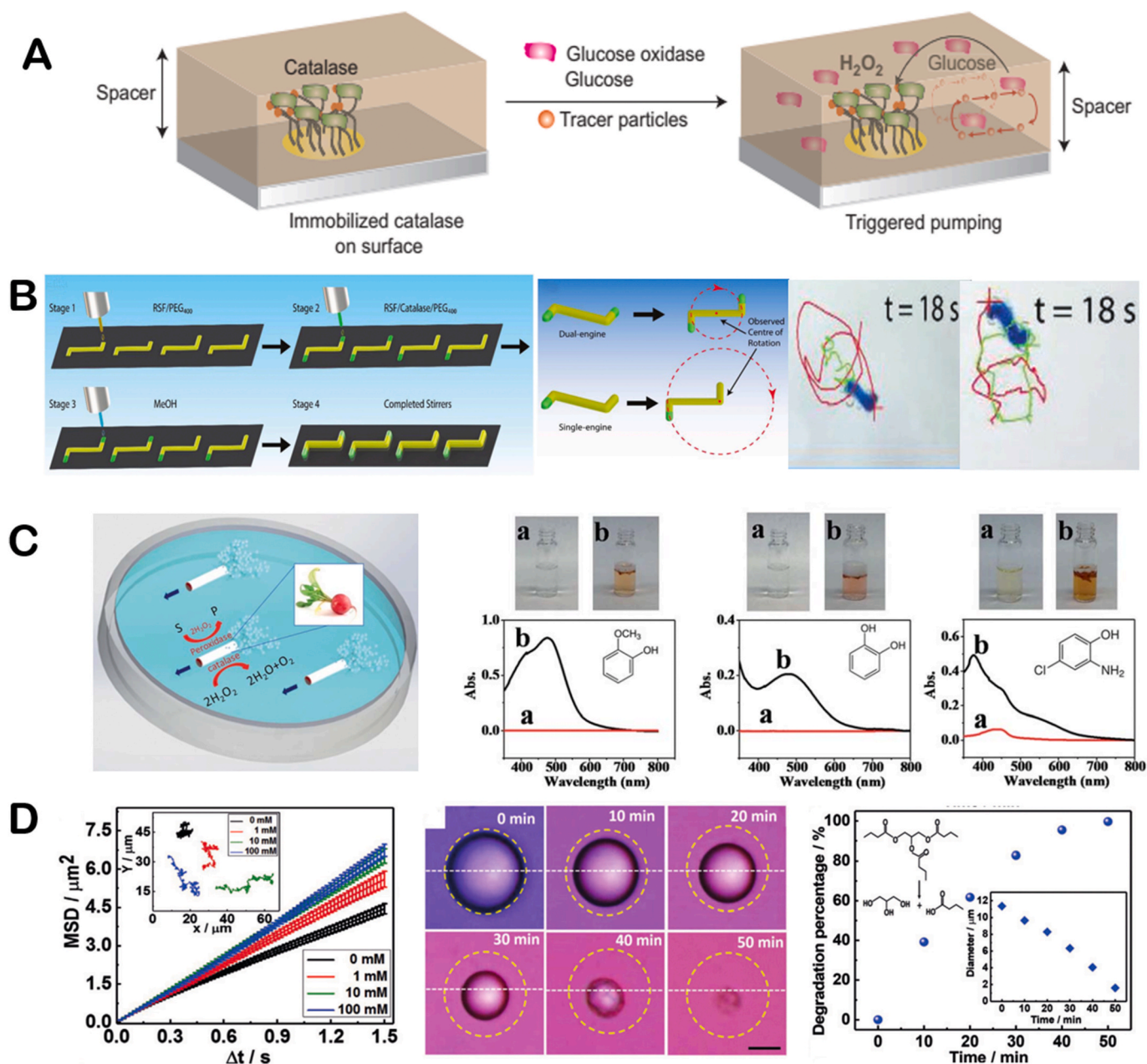


Fig. 13. (A) Illustration of enzymatic micropumps. Reproduced with permission from ref 128. Copyright 2014, Nature. (B) The fabrication of functional silk stirrers using reactive inkjet printing, the rotation center of dual-engine and single-engine silk stirrers during stirring action, still video frames from catalase propelled single-engine stirrers and dual-engine stirrer in the presence of H_2O_2 solutions. Reproduced with permission from ref 131. Copyright 2018, Wiley. (C) Removal of phenolic pollutants by dual-function plant (radish) motors. Reproduced with permission from ref 41. Copyright 2014, Royal Society of Chemistry. (D) Trajectories (inset) and corresponding MSD plot of lipase-powered nanomotors at different triacetin concentrations, the color change of the surrounding litmus solution along time indicates the generation of butyric acid (scale bar: $5 \mu m$), degradation percentage of tributyrin droplets by lipase powered motors at different times. Reproduced with permission from ref 50. Copyright 2019, Wiley.

balance, introducing an extra charge density and an electric field, which create an asymmetric electrostatic force density to propel the particles. The theoretical results quantitatively explained the dependence of the urease-driven colloids velocity on the electrolyte concentration.

In 2005, Golestanian and co-workers proposed a reaction-driven propulsion model, in which the motion of the object was driven by the asymmetric distribution of reaction products [13]. Therefore, the self-propelled motors with asymmetric structures have been developed such as the Janus motors driven by enzyme catalysis. Schattling and co-workers constructed a colloidal motor of the Janus particle that one hemisphere was modified with catalase and GOx [56]. The enhanced diffusion behavior of the colloid motor depending on glucose

concentration was confirmed in buffer solution and multi-component protein solution. The researchers also pointed out that the small swimmers require to breaking the symmetry of the surface activity to generate a gradient and phoretic mobility. Sánchez's group reported the Janus nanomotors that driven by biocatalytic reactions with three different enzymes: catalase, urease and glucose oxidase based on the hollow mesoporous silica nanoparticles (HMSNPs) [47]. From DLS results and MSD analysis, it can be confirmed that Janus nanomotors exhibit enhanced diffusion and the authors suggested that the Janus nanomotors were propelled by a chemo-phoretic mechanism. And for the first time, they used optical tweezers to measure the effective driving force ($F = 64 \pm 16$ fN) that generated by the catalase-powered nanomotor

(Fig. 7C). At the same year, Sen's group prepared enzyme-driven polystyrene microparticles that modified urease and catalase on the surface of the particles with biotin-streptavidin. The results showed that the diffusion of the polystyrene microparticles was enhanced in the presence of its substrate, and the authors explained the diffusion enhancement of these particles was caused by the thermal effect due to exothermic enzymatic reactions [92]. After that, the same group observed the diffusion enhancement of the tracers in the active enzyme solution through FCS and DLS, and suggested that the enhanced diffusion of tracers may be due to the effect of active enzyme on the dynamics of the surrounding environment. The authors also found a similar diffusion behavior in the enzyme solution that catalyzes endothermic reactions, suggesting that the thermal effect is not the main cause of tracer enhanced diffusion [93] (Fig. 7D).

3.2.2. Bubble propulsion mechanism

Another typical mechanism is bubble propulsion, which uses catalase to catalyze the decomposition of hydrogen peroxide to produce oxygen bubbles, similar to the first generation of catalytic motors based on platinum catalysts. In 2010, Sánchez and co-workers reported an efficient hybrid microengine that uses hydrogen peroxide as a fuel and can achieve self-propulsion at very low concentrations [28]. It was showed that the catalase in the cavity of microtube catalyze the decomposition of H_2O_2 to generate oxygen bubbles that propel the hybrid microengine ($H_2O_2 \rightarrow H_2O + 1/2O_2$), and its dynamics was controlled by the production of front-side bubbles (Fig. 8A). Since then, catalase was combined with a variety of micro/nano-carriers to construct the bubble-propelled motors and used in different applications [29, 94–96]. For instance, Wang's group prepared a (PEDOT)/Au-catalase tubular microengine that was driven by bubble propulsion to test water quality [29]. Sitt and co-workers fabricated a biocompatible and biodegradable hollow microtubule, the inner walls of which were modified with catalase. It is confirmed that the catalase-modified microtubules can be used as microrockets driven by bubbles and have potential applications in biomedicine [94] (Fig. 8B). Other researchers have also reported the potential of bubble-propelled nanomotors for cancer therapy [33,35]. Besides, Ma and co-workers constructed a bio-catalytic Janus motor based on the mesoporous silica cluster [97]. The catalase was anchored to the side of the asymmetric sphere, where the oxygen bubbles form rapidly during the catalytic reaction and propelled the bio-catalytic Janus motor towards the non-enzymatic side (Fig. 8C). Wilson's group showed the formation of oxygen bubbles after adding H_2O_2 to catalase-modified nanotubes, and presented the variation of diffusion coefficient with the concentration of H_2O_2 [14] (Fig. 8D).

Moreover, researchers often used a cascade of GOx and catalase to boost the bubble propulsion. For example, Feringa's group covalently linked GOx and catalase on the carbon nanotubes, which were driven by the formation of bubbles. It showed that the glucose was catalyzed by GOx to produce hydrogen peroxide, which was decomposed by catalase to generate oxygen bubbles which drive MWCNTs [55] (Fig. 8E). It is suggested that co-immobilization of GOx and catalase could temporarily increase the oxygen concentration, thereby allowing the formation of oxygen bubbles and moving the nanotube objects through this process. Wilson's group developed a bowl-shaped polymer motor with an opening. They incorporated two complementary enzymes (GOx and catalase) into the cavity of polymeric stomatocytes through a shape-changing process of the polymersomes, and the self-propulsion was achieved by gas expulsion from the opening structure [33,57].

3.2.3. Chemotaxis mechanism of EMNMs

The chemotactic behavior is another important characteristic of EMNMs. In nature, chemotaxis is the directional movement of biological species in response to a gradient in the distribution of chemicals in the environment. For example, it's important for bacteria to find food (such as glucose), so they can move closer to higher concentrations. The study

by Sen's group in 2010 reported the catalysis-enhanced diffusion of urease as the substrate concentration increased. These results showed that the diffusion behavior of the enzyme was highly concentration dependent, and also anticipated that enzymes would exhibit collective behavior of directed movement in the presence of substrate gradient [80]. Then, the same research team utilized urease and catalase to confirm the experimental results, which tended to move towards high substrate concentrations as a new form of molecular chemotaxis [25] (Fig. 9A). Based on the chemotaxis model proposed by Schurr and co-workers [98], the chemotaxis of EMNMs can be accounted by thermodynamically advantageous enzyme-substrate interaction, which leads to the movement towards the concentration gradient of substrate [74]. And the chemotactic property was also shown in the enzymatic cascade reactions. Enzymes have been shown to assemble into metabolon in the presence of the initial substrate. Each enzyme independently follows the gradient of substrate that generated by the previous enzymatic reaction, which may be also due to the chemotaxis effect [99,100]. Using the chemotaxis behavior of the enzyme motors, researchers managed to separate the active enzyme from inactive substances with similar size and charge through the multi-channel microfluidic device [101]. And the chemotaxis of enzyme was further supported in paper-based analytical device [102]. In addition, Mohajerani and co-workers developed a general model to quantitatively understand chemotactic behavior of enzymes in their substrate concentration gradient. The theoretical model and experimental results showed that the substrate-enzyme binding and catalytic turnover enhanced the chemotaxis of enzymes [103] (Fig. 9B).

The scientists predicted that the chemotactic behavior would occur in EMNMs. In the presence of concentration gradient, the directional movement of the active particles can also be regarded as chemotactic behavior. Taking advantage of the three-inlet microfluidic architecture, Sen's group demonstrated that enzyme-driven polystyrene microparticles showed a tendency of chemotaxis and moved towards the regions with higher substrate concentration [92]. Recently, Wilson's group reported the chemotaxis of self-propelled PLGA motors that response to inflammation. The PLGA motors moved in a self-propelling direction along a hydrogen peroxide concentration gradient that was produced by stimulating macrophages. It is suggested that self-propelled drug carriers could fulfill targeted delivery to lesions with elevated H_2O_2 levels, offering promising applications in the treatment of diseases such as rheumatoid arthritis and cancers [104].

However, there are still some differences in the chemotaxis behavior of enzyme motors. The anti-chemotactic behavior (or negative chemotaxis) of urease and acetylcholinesterase that migrate into lower substrate concentration was reported. The authors explained that the anti-chemotactic behavior is caused by stochastic leap of active enzymes [105] (Fig. 9C). Golestanian's group proposed two competitive mechanisms of enzyme chemotaxis, the diffusion phoretic mechanism due to the nonspecific interactions and the enhanced diffusion induced by binding [87]. The chemotaxis mechanism of the former leads to positive chemotaxis, while the latter leads to antichemotaxis. They also found that phoresis plays a dominant role with the substrate above critical concentration, while the binding-induced diffusion enhancement plays a dominant role at a low substrate concentration (Fig. 9D). The relationship between enhanced diffusion and the chemotaxis of enzymes was presented. Besides, Somasundar and co-workers recently found that the direction of chemotactic behavior of enzyme-coated liposome motors can be regulated, both positive and negative chemotaxis of enzyme-coated liposome motors was demonstrated [106] (Fig. 9E). In this study, liposome motors coated with catalase exhibited positive chemotactic behavior, liposome motors coated with urease exhibited negative chemotactic behavior, and those coated with ATPase had both positive and negative chemotaxis. Through experimental exploration and testing, the authors suggested that the propulsion mechanism of enzyme-coated liposome motors was based on the competition between enzymatic-induced positive chemotaxis and

solute-phospholipid-interaction-based negative chemotaxis. And it was showed that the movement direction of ATPase-coated liposomes could be regulated by the concentration of the substrate ATP.

3.3. Affecting factors of EMNMs

The motion of EMNMs was affected by many parameters, for instance, the size or shape of the synthetic structures, the intrinsic property of enzymes, and the quantity and distribution of immobilized enzymes. For the tubular enzyme-powered motor, the propulsion speed of the motors was often closely related to diameter of the tubular [29, 94], similarly, for the spherical structure, the diameter greatly affects the motion dynamics. Compared to the micro-scaled particles, the nano-scaled particles experienced higher interference by Brownian motion and displayed the enhanced diffusion behavior [62].

Chen and co-workers fabricated a catalase-powered microshell motors with different sizes of multimetallic (Au/Ag/Au) microshells and studied the motion behavior of the microshell motors [107]. As shown in Fig. 10A, microshells with a size smaller than 5 μm displayed a slow trembled movement because of the low efficiency of bubble generation and weak driving force. Meanwhile, microshells larger than 5 μm have the high efficiency of bubble generation, and showed that fast translational motion with strong driving force. It is suggested that the motion speed and behavior were not only size-dependent, but also affected by the efficiency of bubble generation and the ejection way of bubbles. Although the larger size of motors can produce faster translational motion, the smaller size of nanomotor that can move *in vivo* have the advantage of overcoming the biological barriers when applied in biomedicine, especially for tumor therapy. Wilson's group developed nano-scaled motors with the size of around 400 nm and 150 nm for *in vivo* cancer therapy application. Comparing the two sizes of nanomotors, the ultrasmall stomatocyte motor have higher penetrability in vasculature model. And it is found that the moving velocity of the motor is correlated to the fuel concentration, the motor speed increased with the O_2 production [33]. Nakata and co-workers demonstrated the increase of hydrogen peroxide concentration resulted in irregular oscillation motion, periodic oscillation motion and continuous motion of the self-propelled motors. The results showed that the motion of self-propelled motors depended on an enzymatic reaction and the production dynamics of O_2 bubbles [108].

Additionally, regardless of their size, the asymmetric distribution of catalysts has been considered necessary for the generation of active motion. Most of the works have modified the enzyme on one side of the Janus structure to achieve asymmetric distribution of enzymes. However, recent studies showed that the non-Janus spherical enzyme-powered motor also exhibited the enhanced diffusion behavior. Sen's group coated the polystyrene particles with enzymes that exhibited the enhanced diffusion behavior [92]. Ma and co-workers fabricated a hollow SiO_2 motors where the non-Janus structure has a natural asymmetry due to the presence of a hole on its surface and propelled by enzyme [90]. Sánchez's group investigated the effects of the distribution and number of enzymes on the motion of non-Janus motors. It is shown that the enzyme was distributed on the surface of PS or PS@ SiO_2 in non-uniform form. They revealed that the directional propulsion speed of PS@ SiO_2 motors is higher than the PS-based motors, because of the presence of a large number of enzymes on surface of the PS@ SiO_2 motor (Fig. 10B). Besides, the number of enzymes influenced the speed and force produced by PS@ SiO_2 micromotors. The authors demonstrated that the enzymes as patches distribute on the surface of micromotor and there is a certain threshold number of enzymes to produce active motion [109]. Wilson's group fabricated the enzyme-based hydrogel microparticles with an opening shape by using microfluidic chip. They investigated the influence of the opening surface roughness on the speed of the motor. And found that the motor with surface roughness could be easier to pin oxygen bubbles and control speed better than a motor with less rough surface [32]. In addition, Ma and co-workers had

demonstrated that the distribution of enzymes can also regulate the movement of the motor. The authors selectively modified urease on inside, outside, or all over the nanotube to investigate the effect of urease distribution on the motion of tubular nanojets. The result showed that the enzyme located inside is responsible for self-propulsion movement and that located outside nanojets contribute to the speed enhancement [42] (Fig. 10C). Recently, Guan and co-workers reported a novel approach to boost the propulsion force of urease-driven motors by assembling multilayered urease on Janus magnetic microparticles to increase the number of enzymes [110]. The results showed that the migration speed of multilayered urease-driven micromotors was about 5 times faster than that of the monolayered counterparts because of the multilayered surface with much more catalytic units.

In the second part of this review paper, many types of enzymes are used to drive micro/nano-structures. It is known that different enzymes possess different enzyme kinetics, which would influence the motion dynamics of EMNMs. Therefore, the intrinsic properties of enzymes are important factors that influence the motion of EMNMs. For instance, the catalytic activity (K_{cat}) of the enzyme is the most critical characteristic. Generally speaking, the enzyme with higher catalytic activity would yield stronger driving force. In this sense, Ma and co-workers conjugated catalase, urease, and GOx, respectively, on the HMSNPs to propel the nanomotors [47]. It was observed that the catalase-based nanomotor showed highest motion effect corresponding to highest reaction rate among the three motors, suggesting the enhanced diffusion was related to the catalytic activity of the enzyme. And then, the authors used inhibitors to regulate enzyme activity. They fabricated a urease-powered Janus motor that motion can be controlled by chemical inhibitors ($\text{Ag}^+/\text{Hg}^{2+}$) and reactivator (DTT). The Ag^+ or Hg^{2+} would stop the motor, while the DTT would restart the motor movement [15] (Fig. 10D). Furthermore, Arqué and co-workers analyzed the motion speed of silica microcapsules driven by urease, glucose oxidase, acetylcholinesterase, and aldolase. They studied how the turnover number and conformational dynamics of these four enzymes affect their self-propulsion behavior, showing that the diffusion increased with the turnover number. It proved that the crucial role of catalytic efficiency of enzymes for EMNMs [111] (Fig. 10E).

4. Practical applications of EMNMs

4.1. Biomedical application of EMNMs

Due to their biocompatibility and controlled motion, EMNMs bring unique improvement for biomedical applications ranging from target drug delivery to photodynamic therapy, *etc.* Hortelão and co-workers fabricated urease powered silica-based nanobots to achieve enhanced drug delivery efficiency compared to passive carries [43]. Uncontrolled drug release in conventional drug delivery often lead to drug leakage that may cause serious toxic and side effects. The intelligent controllable drug delivery system can respond to the stimulation of external environment such as pH, temperature, light, oxidant, *etc.* and selectively release drugs to targeted sites and consequently improve the drug delivery efficiency. For example, He's group constructed catalase driven microrockets by incorporating thermal sensitive gelation hydrogel into the poly-L-lysine/bovine serum albumin (PLL/BSA) multilayer microtubes [112]. The movement of the micromotors through enzymatic bubble propulsion increased the speed of drug delivery. Subsequently the phase transition of gelatin hydrogel under near-infrared light irradiation empowered microrockets the ability to release drugs in specific sites and effectively kill the surrounding cancer cells (Fig. 11A). They also exploited light responsive polymer capsules motors propelled by catalase for controlling drug delivery towards cancer cells [96]. Quite a few works reported EMNMs that can realize stimuli-responsive drug delivery in response to microenvironment conditions of tumors (low pH and elevated glutathione levels). Lorente and co-workers developed enzymatic nanomotors for intracellular payload delivery. The

nanomotors were composed of mesoporous silica nanoparticles gated with benzimidazole: cyclodextrin modified urease (CD-U) nanovalves [44]. Drugs or dyes loaded in these nanomotors could be released on command under acidic condition, in which the benzimidazole groups were in protonation and then the benzimidazole: CD-U nanovalves disintegrated. In addition, the nanomotors based on Janus Au-mesoporous silica nanoparticles for glutathione-responsive controlled drug release in the specific sites also were prepared [113]. In this work, the gold face of the Janus nanomotors was grafted with catalase, and the silica face of the Janus nanomotors was used for drug loading and wrapped with disulfide-linked oligo (ethylene glycol) (SS-OEG) chains. The nanomotors performed autonomous motion in the presence of H_2O_2 . Then the reduction of SS-OEG chains by glutathione triggered the release of cargo (Fig. 11B). Furthermore, Gao and co-workers assembled pH-sensitive β -lactoglobulin and catalase into the porous framework particles [37]. The biocatalytic micromotors can serve as pH responsive drug carriers at ultralow H_2O_2 concentration.

In another aspect, EMNMs based drug delivery system need to overcome multiple physiological and pathological barriers [114]. These barriers directly affect the outcome of the treatment. To maximize drug delivery efficacy, the EMNMs that are applied for drug delivery have been designed to overcome some of these biological barriers. Walker and co-workers immobilized urease onto the surface of magnetic micropellers for the penetration of mucin gels through mimicking bacterium *Helicobacter pylori* [115]. In the presence of substrate urea, products catalyzed by urease could increase the pH of environment to change the fluid properties of mucus and consequently improved the penetration of micromotors. Wang and co-workers encapsulated GOx or/and Cat into the asymmetric polymersome which easily combined with peptides that target LRP-1 (low-density lipoprotein receptor-related protein 1). Driven by enzymatic decomposition of glucose, the asymmetric polymersome presented chemotaxis behavior and enhanced ability of crossing blood brain barrier [116] (Fig. 11C). The urease propelled mesoporous silica based nanomotors, coupled with anti-FGFR3 that can target the bladder cancer cells and inhibit proliferation of cancer cells, were shown to significantly improve therapeutic effect against bladder cancer [117] (Fig. 11D). Recently, Tang and co-workers developed cellular robots by asymmetric functionalization of platelet surface with urease. When exposed to a natural fuel (urea), urease-driven cellular machinery greatly accelerates platelets' specific adherence to target cells and thus increases drug delivery efficiency [118]. The strategy to overcome cellular barriers by reducing the size of enzymatic motors were reported by Sun and co-workers. They prepared ultrasmall stomatocyte polymersomes (150 nm) encapsulating catalase and found that the nanomotors could obtain the enhanced penetration capability for the vasculature model in low concentration of H_2O_2 [34]. Besides, Li and co-workers also reported that tadpole-like asymmetry nanomotors (100 nm) constructed by using a single molecular bottle-brush and catalase. The nanomotors exhibited efficient directional propulsion in a viscous tumor microenvironment of gel model and demonstrated potential for tissue penetration [35]. Chen and co-workers loaded urease powered nanomotors into electrospun fiber fragments, so that the nanomotors could be lunched from intertumoral depots to overcome the biological barriers in the drug delivery pathway [119].

As a mobile carrier of photosensitizer, Ma's group used enzymatic motors for photodynamic therapy against bacteria. They constructed urease powered micromotors composed of photosensitizer and magnetic nanoparticles on the surface of hollow mesoporous SiO_2 microspheres [90]. This photosensitizer platform based on the enzymatic micromotors presented enhanced photodynamic therapy for anti-bacteria by promoting exposure between 3O_2 and photosensitizer and improving the diffusion of toxic 1O_2 (Fig. 11E). Recently, they also prepared enzymatic nanomotors by loading GOx and catalase on upconversion nanoparticles@zeolitic imidazolate framework-8 (UCNP@ZIF-8) capped with photosensitizer. The dual enzyme propelled nanomotors promoted synergistic photodynamic therapy and starvation therapy, which

resulted from glucose consumption and oxygen generation by enzymatic cascade reaction [59].

4.2. Biochemical and environmental sensing

EMNMs have been applied to biochemical sensing based on a variety of analytical signals (moving speed, color and fluorescence change). Motion-based sensing strategies have shown its potential in analytical science because they do not require sophisticated instruments and thus are suitable for point-of-care diagnosis. For instance, by analyzing the motion behavior, EMNMs were reported to be able to detect enzyme inhibitors, catalytic substrate and DNA [29,30,95,120–124]. Wang's group modified polymeric PEDOT/Au bilayer microtubes with catalase for testing toxic pollutants in water including NaN_3 , Hg, Cu and aminotriazole [29]. The movement speed of PEDOT/Au-catalase tubular micromotors through bubble propulsion was correlated to the inhibited activity of catalase by toxic substances. Thus, the motion speed could reflect the concentration of toxic substances (Fig. 12A). Nerve-agent vapor that can inhibit the bio-catalytic activity of catalase was also detected by monitoring the change of motion speed of catalase powered motors [120]. Using the same mechanism as above, Rivera and co-workers developed enzyme-powered pumps and used the fluid velocity of micropumps measured by optical tracking of tracer particles to analyze the concentration of mercuric, cadmium, cyanide, and azide ions that inhibit enzyme catalytic reactions [121] (Fig. 12B). It is well known that the concentration of enzymatic substrate is closely related to the motion of EMNMs. So, Bunea and co-workers detected the corresponding catalytic substrate concentration of glucose, glutamic acid or hypoxanthine by measuring the diffusion coefficient of nanorods decorated with glucose oxidase (GOx), glutamate oxidase (GluOx), or xanthine oxidase (XOD) [122]. Simmchen and co-workers immobilized single strand DNA and catalase on each face of a Janus silica particle, to construct asymmetrical nanomotor. The DNA functionalized nanomotors and DNA modified cargo particles were linked through hybridization of the two complementary DNA strands. Therefore target DNA was detected by tracking the movement of larger cargo particles linked with nanomotors [123]. In another work, Wu's group designed PEDOT/Au microtubes with catalase assembled through DNA coupling for sensing target DNA based on motion speed [124]. The target DNA could replace the single strand DNA conjugated with catalase, resulting in the decrease of the number of enzyme immobilized on micromotors and therefore the decrease of motion speed of the micromotors (Fig. 12C). Subsequently, multiple layers of catalase were decorated on the inner surface of PEDOT-PSS/Au micromotors and multi-metallic (Au/Ag/Ni/Au) jellyfish-like micromotors through DNA assembly to improve the detecting sensitivity of target DNA [30,95].

The integration of colorimetric and fluorescent sensing into EMNMs could simplify the analysis process and improve the detection efficiency. Russell and co-workers combined micromotors and competitive immunoassay to detect sepsis biomarker procalcitonin through color change, which could be quantified through relative pixel intensity of camera equipped in a smartphone [125]. In this work, procalcitonin and procalcitonin conjugated catalase competitively bonded with iron oxide particles through antibodies to form enzyme powered micromotors. Thus, the concentration of procalcitonin would affect the amount of enzyme conjugated on iron oxide particles which was closely related to the motion of EMNMs. Thanks to the color of iron oxide particles, change of motion was converted to color variation on filter paper which was used to quantify procalcitonin (Fig. 12D). Patino and co-workers decorated the urease-powered micromotors with FRET-labeled pH-sensitive DNA nanoswitches for real-time monitoring pH of the surrounding micro-environment. In addition, the activity of micromotors could be simultaneously monitored through confocal laser microscopy observation [126] (Fig. 12E). During the propulsion of micromotors, the ammonia generated from the decomposition of urea could increase the pH of the micro-environment around the motors and thus changed the

FRET efficiency. Furthermore, a Janus micromotor was reported for ratiometric fluorescent sensing of circulating tumor cells (CTCs). Catalase and aptamer conjugated with tetraphenylethene (TPE) and fluorescein isothiocyanate (FITC) were decorated on the both side of Janus rods, respectively [127]. Aggregation-induced emission (AIE) effect of TPE and aggregation-caused quenching (ACQ) phenomenon of FITC on micromotors disappeared because the binding of CTCs with aptamer caused the unbinding of TPE and FITC from micromotors. As a result, motion of the micromotors imposed the advantages of the rapid recognition and low detection limit for CTCs.

4.3. Other applications of EMNMs

Enzyme powered micropumps, where enzyme catalytic reactions transfer chemical energy to the flow of surrounding fluid, can precisely control the flow rate and directions in response to external stimuli. Sen's group developed multiple enzyme powered micropumps which could be propelled by DNA polymerase [26], catalase, lipase, urease, glucose oxidase [121,128–130], phosphatase [49]. For instance, they initially immobilized several ATP-independent enzyme (catalase, lipase, urease, glucose oxidase) on the surface of quaternary ammonium thiol functionalized Au to construct micropumps [128] (Fig. 13A). The micropump could be triggered in the presence of catalytic substrate and flow rate can be controlled by substrate concentration. For the potential of practical applications, enzyme powered micropumps without external power source might pave new way to the design of portable and smart microfluidic devices. Furthermore, the bio-catalytic pumps can be used for cargo delivery, such as transporting insulin [128], microparticles [129] to targeted regions within the microchamber.

In order to improve the mixing effect in biochemical sensing, reactive inkjet printing was reported to fabricate silk-based microstirrers that allow for rapid fluid mixing in small volumes [131]. The authors designed two types of stirrers driven by enzymatic reaction and Marangoni effect. The enzyme powered stirrers showed increased lifespan of the mixing, which was helpful for the point-of-care analysis (Fig. 13B).

Moreover, biocatalytic micromotors have been used for “on the fly” environmental remediation due to their motion ability [41,50]. Satayasamitsathit and co-workers firstly developed cost-effective biomotors based on plant tissues of *Raphanus sativus* for improved removal of phenolic pollutants. The catalase and peroxidase could accelerate both the movement of motors and the conversion of phenolic contaminants. Consequently, the removal of pollution reached maximum in 3 min and the decontamination efficiency of toxic phenolic was enhanced greatly [41] (Fig. 13C). Wang and co-workers developed silica-based nanomotors functionalized by lipase which plays the roles of power engine and cleaner for tributyrin. The developed nanomotors performed enhanced diffusion for up to 40 min in the presence of triacetin (<10 mM) and facilitated the degradation of triglyceride [50] (Fig. 13D).

5. Summary and outlook

In this review, we introduced the classification of EMNMs, self-propulsion mechanism and the applications of EMNMs. The introduction of enzymes has greatly promoted the development of EMNMs, from ATPases that can move autonomously in cells to artificially-synthesized EMNMs, all of which are benefiting from natural enzymatic reactions with regarding to the biocompatibility, energy conversion efficiency, etc. Scientists have synthesized a variety of EMNMs based on different materials and micro/nano-structures. Utilization of different enzymes makes EMNMs achieve new functions that are capable of accomplish on-demand tasks. For instance, the invention of bio-degradable and/or biocompatible EMNMs consuming non-toxic fuel enables much more bio-friendly micro/nano motors for nanomedicine applications. The cascade reaction of oxide GOx and catalase is of great significance by converting fuel from biologically toxic hydrogen peroxide to physiologically available glucose. Although the research on EMNMs has

obtained considerable achievements including even *in vivo* attempts in biomedicine, it is still facing quite a lot of apparent challenges, as most of currently applications of EMNMs are proof-of-concept demonstrations within laboratory.

Although there are still debate on the fundamental knowledge about self-propulsion process of EMNMs, it is undeniable that the propulsion force of EMNMs is generated by the bio-catalytic reaction of immobilized enzymes on micro/nano-structures. Scientists have done a lot of work to reveal the propulsion mechanism of EMNMs, including insights into the fundamental mechanism of single enzyme movement and synthetic EMNMs. The description of the motion behavior of EMNMs mainly involved the enhancement of Brownian diffusion, the classical bubble propulsion, phoretic mechanism and chemotactic behavior. Moreover, the motion of EMNMs was regulated by many factors such as the size, fuel concentration, the number and intrinsic properties of enzymes. However, there are still controversies about the propulsion mechanism of single enzyme and enzyme-driven machines. At present, aiming at practical applications in various fields, EMNMs need to improve their propulsive force to overcome resistance brought by complicated surrounding environment. The current methods to improve the driving force include changing the shape of motors to accommodate the hydrodynamics, increasing the catalytic capacity of the enzymes (e. g. increasing the catalytic unit of enzymes), and using the cascade reaction which have two or more enzymes for propelling. In the future, in addition to currently reported strategies, more advanced analytical or testing techniques should be introduced to verify the energy conversion mechanism that generate propulsion force by enzymatic reactions, which would give fundamental and theoretical guidance on future development of highly efficient EMNMs with stronger propulsion capability.

We thoroughly reviewed up-to-date various proof-of-concept applications of EMNMs, such as biomedical therapy, biochemical sensing, environmental remediation, as well as microfluidic pumping. The biocompatibility of EMNMs endows great potential for replacing traditional inorganic catalyst-based MNMs to solve toxic challenges in biomedicine use. However, the complex biological environment (high viscosity, strong blood flow, complicated chemical and biological components) will bring great difficulties to the biological applications of EMNMs, at least but not limited to the stability of the enzymatic activities and their motion capability. Therefore, future investigation can be aiming at these challenges in order to realize efficient movement in realistic biological environment and moving towards practical clinic use of EMNMs in future. Furthermore, nature provides an extremely large pool of enzymes which are widely existing in living organisms. Up to now, studies on EMNMs are limited to only a few commonly known enzymes. Researchers should pay extra attentions to many other unexplored enzymes/fuels combinations to develop new EMNMs consuming different fuels. In most of proof-of-concept applications of EMNMs, the enzymes are only serving as power supply by converting chemical energy into mechanic self-propulsion force. However, enzymes possess many important biofunctions in nature. Taking advantage of the intrinsic functionalities of enzymes will be able to greatly expand the potential applications of EMNMs.

Declaration of competing interest

The authors declare no competing financial interest.

Acknowledgements

The authors thank the financial support from the National Natural Science Foundation of China (51802060), Shenzhen Science and Technology Program (KQTD20170809110344233), Shenzhen Bay Laboratory (SZBL2019062801005), and Natural Science Foundation of Guangdong Province (No. 2019A1515010762).

References

- [1] R. Mhanna, F. Qiu, L. Zhang, Y. Ding, K. Sugihara, M. Zenobi-Wong, B.J. Nelson, Artificial bacterial flagella for remote-controlled targeted single-cell drug delivery, *Small* 10 (2014) 1953–1957.
- [2] D. Kagan, M.J. Benichmol, J.C. Claussen, E. Chuluun-Erdene, S. Esener, J. Wang, Acoustic droplet vaporization and propulsion of perfluorocarbon-loaded microbullets for targeted tissue penetration and deformation, *Angew Chem. Int. Ed. Engl.* 51 (2012) 7519–7522.
- [3] W. Xi, A.A. Solovlev, A.N. Ananth, D.H. Gracias, S. Sanchez, O.G. Schmidt, Rolled-up magnetic microdrillers: towards remotely controlled minimally invasive surgery, *Nanoscale* 5 (2013) 1294–1297.
- [4] B. Esteban-Fernández de Ávila, A. Martín, F. Soto, M.A. Lopez-Ramirez, S. Campuzano, G.M. Vasquez-Machado, W. Gao, L. Zhang, J.J.A.N. Wang, Single cell real-time miRNAs sensing based on nanomotors, *ACS Nano* 9 (2015) 6756–6764.
- [5] C. Liang, C. Zhan, F. Zeng, D. Xu, Y. Wang, W. Zhao, J. Zhang, J. Guo, H. Feng, X. Ma, Bilayer tubular micromotors for simultaneous environmental monitoring and remediation, *ACS, Appl Mater Interfaces* 10 (2018) 35099–35107.
- [6] H. Wang, B. Khezri, M.J.C. Pumera, Catalytic DNA-functionalized self-propelled micromachines for environmental remediation 1 (2016) 473–481.
- [7] S. Sanchez, L. Soler, J. Katuri, Chemically powered micro- and nanomotors, *Angew Chem. Int. Ed. Engl.* 54 (2015) 1414–1444.
- [8] W. Gao, A. Pei, J. Wang, Water-driven micromotors, *ACS Nano* 6 (2012) 8432–8438.
- [9] M. Ibele, T.E. Mallouk, A. Sen, Schooling behavior of light-powered autonomous micromotors in water, *Angew Chem. Int. Ed. Engl.* 48 (2009) 3308–3312.
- [10] J.J. Kwan, R. Myers, C.M. Coviello, S.M. Graham, A.R. Shah, E. Stride, R. C. Carlisle, C.C. Coussios, Ultrasound-propelled nanocaps for drug delivery, *Small* 11 (2015) 5305–5314.
- [11] T. Li, J. Li, K.I. Morozov, Z. Wu, T. Xu, I. Rozen, A.M. Leshansky, L. Li, J. Wang, Highly efficient freestyle magnetic nanoswimmer, *Nano Lett.* 17 (2017) 5092–5098.
- [12] D. Fan, Z. Yin, R. Cheong, F.Q. Zhu, R.C. Cammarata, C.L. Chien, A. Levchenko, Subcellular-resolution delivery of a cytokine through precisely manipulated nanowires, *Nat. Nanotechnol.* 5 (2010) 545–551.
- [13] R. Golestanian, T.B. Liverpool, A. Ajdari, Propulsion of a molecular machine by asymmetric distribution of reaction products, *Phys. Rev. Lett.* 94 (2005) 220801.
- [14] B.J. Toebes, L.K.E.A. Abdelmohsen, D.A. Wilson, Enzyme-driven biodegradable nanomotor based on tubular-shaped polymeric vesicles, *Polym. Chem.* 9 (2018) 3190–3194.
- [15] X. Ma, X. Wang, K. Hahn, S. Sanchez, Motion control of urea-powered biocompatible hollow microcapsules, *ACS Nano* 10 (2016) 3597–3605.
- [16] D.S. Tsao, M.R. Diehl, Molecular motors: myosins move ahead of the pack, *Nat. Nanotechnol.* 9 (2014) 9–10.
- [17] M.J. Tyska, D.M. Warshaw, The myosin power stroke, *Cell Motil Cytoskeleton* 51 (2002) 1–15.
- [18] M.A. Welte, Bidirectional transport along microtubules, *Curr. Biol.* 14 (2004) R525–R537.
- [19] E. Toprak, A. Yildiz, M.T. Hoffman, S.S. Rosenfeld, P.R. Selvin, Why kinesin is so processive, *Proc. Natl. Acad. Sci. U.S.A.* 106 (2009) 12717–12722.
- [20] M. Yoshida, E. Muneyuki, T. Hisabori, ATP synthase - a marvellous rotary engine of the cell, *Nat. Rev. Mol. Cell Biol.* 2 (2001) 669–677.
- [21] H. Noji, R. Yasuda, M. Yoshida, K. Kinosita, Direct observation of the rotation of F₁-ATPase, *Nature* 386 (1997) 299–302.
- [22] H. Noji, Amersham Pharmacia Biotech, Science Prize, - the rotary enzyme of the cell: the rotation of F₁-ATPase., *Science* 282 (1998) 1844–1845.
- [23] C. Montemagno, G. Bachand, Constructing nanomechanical devices powered by biomolecular motors, *Nanotechnology* 10 (1999) 225–231.
- [24] H.S. Muddana, S. Sengupta, T.E. Mallouk, A. Sen, P.J. Butler, Substrate Catalysis Enhances Single-Enzyme Diffusion, *J Am Chem Soc* 01 (2010) 2110–2111.
- [25] S. Sengupta, K.K. Dey, H.S. Muddana, T. Tabouillot, M.E. Ibele, P.J. Butler, A. Sen, Enzyme molecules as nanomotors, *J. Am. Chem. Soc.* 135 (2013) 1406–1414.
- [26] S. Sengupta, M.M. Spiering, K.K. Dey, W. Duan, D. Patra, P.J. Butler, R. D. Astumian, S.J. Benkovic, A. Sen, DNA polymerase as a molecular motor and pump, *ACS Nano* 8 (2014) 2410–2418.
- [27] A.-Y. Jee, Y.-K. Cho, S. Granick, T. Tlustý, Catalytic enzymes are active matter, *Proc. Natl. Acad. Sci. U.S.A.* 115 (2018) E10812–E10821.
- [28] S. Sanchez, A.A. Solovlev, Y. Mei, O.G. Schmidt, Dynamics of biocatalytic microengines mediated by variable friction control, *J. Am. Chem. Soc.* 132 (2010) 13144–13145.
- [29] J. Orozco, V. García-Gradilla, M. D'Agostino, W. Gao, A. Cortés, J. Wang, Artificial enzyme-powered microfish for water-quality testing, *ACS Nano* 7 (2013) 818–824.
- [30] S. Fu, X. Zhang, Y. Xie, J. Wu, H. Ju, An efficient enzyme-powered micromotor device fabricated by cyclic alternate hybridization assembly for DNA detection, *Nanoscale* 9 (2017) 9026–9033.
- [31] H. Fang, J. Chen, L. Lin, F. Liu, H. Tian, X. Chen, A strategy of killing three birds with one stone for cancer therapy through regulating the tumor microenvironment by H₂O₂-responsive gene delivery system, *ACS Appl. Mater. Interfaces* 11 (2019) 47785–47797.
- [32] S. Keller, S.P. Teora, G.X. Hu, M. Nijemeisland, D.A. Wilson, High-throughput design of biocompatible enzyme-based hydrogel microparticles with autonomous movement, *Angew Chem. Int. Ed. Engl.* 57 (2018) 9814–9817.
- [33] J. Sun, M. Mathesh, W. Li, D.A. Wilson, Enzyme-powered nanomotors with controlled size for biomedical applications, *ACS Nano* 13 (2019) 10191–10200.
- [34] X. Ma, S. Sanchez, Bio-catalytic mesoporous Janus nano-motors powered by catalase enzyme, *Tetrahedron* 73 (2017) 4883–4886.
- [35] H. Li, Z. Sun, S. Jiang, X. Lai, A. Bockler, H. Huang, F. Peng, L. Liu, Y. Chen, Tadpole-like unimolecular nanomotor with sub-100 nm size swims in a tumor microenvironment model, *Nano Lett.* 19 (2019) 8749–8757.
- [36] B.V.V.S.P. Kumar, A.J. Patil, S. Mann, Enzyme-powered motility in buoyant organoclay/DNA protocells, *Nat. Chem.* 10 (2018) 1154–1163.
- [37] S. Gao, J. Hou, J. Zeng, J.J. Richardson, Z. Gu, X. Gao, D. Li, M. Gao, D.-W. Wang, P. Chen, V. Chen, K. Liang, D. Zhao, B. Kong, Superassembled biocatalytic porous framework micromotors with reversible and sensitive pH-speed regulation at ultralow physiological H₂O₂ concentration, *Adv. Funct. Mater.* 29 (2019).
- [38] Z. Guo, T. Wang, A. Rawal, J. Hou, Z. Cao, H. Zhang, J. Xu, Z. Gu, V. Chen, K. Liang, Biocatalytic self-propelled submarine-like metal-organic framework microparticles with pH-triggered buoyancy control for directional vertical motion, *Mater. Today* 28 (2019) 10–16.
- [39] W.S. Jang, H.J. Kim, C. Gao, D. Lee, D.A. Hammer, Enzymatically powered surface-associated self-motile protocells, *Small* 14 (2018), e1801715.
- [40] Y. Gu, S. Sattayasamitsathit, K. Kaufmann, R. Vazquez-Duhalt, W. Gao, C. Wang, J. Wang, Self-propelled chemically-powered plant-tissue biomotors, *Chem. Commun.* 49 (2013) 7307–7309.
- [41] S. Sattayasamitsathit, K. Kaufmann, M. Galarnyk, R. Vazquez-Duhalt, J. Wang, Dual-enzyme natural motors incorporating decontamination and propulsion capabilities, *RSC Adv.* 4 (2014) 27565–27570.
- [42] X. Ma, A.C. Hortelao, A. Miguel-Lopez, S. Sanchez, Bubble-free propulsion of ultrasmall tubular nanofets powered by biocatalytic reactions, *J. Am. Chem. Soc.* 138 (2016) 13782–13785.
- [43] A.C. Hortelão, T. Patiño, A. Perez-Jiménez, À. Blanco, S. Sánchez, enzyme-powered nanobots enhance anticancer drug delivery, *Adv. Funct. Mater.* 28 (2018) 1705086–1705096.
- [44] A. Llopis-Lorente, A. Garcia-Fernandez, N. Murillo-Cremaes, A.C. Hortelao, T. Patiño, R. Villalonga, F. Sancenon, R. Martinez-Manez, S. Sanchez, Enzyme-powered gated mesoporous silica nanomotors for on-command intracellular payload delivery, *ACS Nano* 13 (2019) 12171–12183.
- [45] N. Sugai, Y. Morita, T. Komatsu, Nonbubble-propelled biodegradable microtube motors consisting only of protein, *Chem. Asian J.* 14 (2019) 2953–2957.
- [46] M. Alarcon-Correa, J.P. Gunther, J. Troll, V.M. Kadiri, J. Bill, P. Fischer, D. Rothenstein, Self-assembled phase-based colloids for high localized enzymatic activity, *ACS Nano* 13 (2019) 5810–5815.
- [47] X. Ma, A. Jannasch, U.R. Albrecht, K. Hahn, A. Miguel-Lopez, E. Schaffer, S. Sanchez, Enzyme-powered hollow mesoporous janus nanomotors, *Nano Lett.* 15 (2015) 7043–7050.
- [48] S. Ghosh, F. Mohajerani, S. Son, D. Velegol, P.J. Butler, A. Sen, Motility of enzyme-powered vesicles, *Nano Lett.* 19 (2019) 6019–6026.
- [49] L. Valdez, H. Shum, I. Ortiz-Rivera, A.C. Balazs, A. Sen, Solutal and thermal buoyancy effects in self-powered phosphatase micropumps, *Soft Matter* 13 (2017) 2800–2807.
- [50] L. Wang, A.C. Hortelao, X. Huang, S. Sanchez, Lipase-powered mesoporous silica nanomotors for triglyceride degradation, *Angew Chem. Int. Ed. Engl.* 58 (2019) 7992–7996.
- [51] J. Bath, S.J. Green, A.J. Turberfield, A free-running DNA motor powered by a nicking enzyme, *Angew Chem. Int. Ed. Engl.* 44 (2005) 4358–4361.
- [52] K. Yehl, A. Mugler, S. Vivek, Y. Liu, Y. Zhang, M. Fan, E.R. Weeks, K. Salaita, High-speed DNA-based rolling motors powered by RNase H, *Nat. Nanotechnol.* 11 (2016) 184–190.
- [53] N. Mano, A. Heller, Bioelectrochemical propulsion, *J. Am. Chem. Soc.* 127 (2005) 11574–11575.
- [54] I.-A. Pavel, A.-I. Bunea, S. David, S. Gaspar, Nanorods with biocatalytically induced SelfElectrophoresis, *ChemCatChem* 6 (2014) 866–872.
- [55] D. Pantarotto, W.R. Browne, B.L. Feringa, Autonomous propulsion of carbon nanotubes powered by a multienzyme ensemble, *Chem. Commun.* (2008) 1533–1535.
- [56] P. Schattling, B. Thingholm, B. Städler, Enhanced diffusion of glucose-fueled Janus particles, *Chem. Mater.* 27 (2015) 7412–7418.
- [57] L.K. Abdelmohsen, M. Nijemeisland, G.M. Pawar, G.J. Janssen, R.J. Nolte, J. C. van Hest, D.A. Wilson, Dynamic loading and unloading of proteins in polymeric stomatocytes: formation of an enzyme-loaded supramolecular nanomotor, *ACS Nano* 10 (2016) 2652–2660.
- [58] B.J. Toebes, F. Cao, D.A. Wilson, Spatial control over catalyst positioning on biodegradable polymeric nanomotors, *Nat. Commun.* 10 (2019) 5308.
- [59] Y. You, D. Xu, X. Pan, X. Ma, Self-propelled enzymatic nanomotors for enhancing synergetic photodynamic and starvation therapy by self-accelerated cascade reactions, *Applied Materials Today* 16 (2019) 508–517.
- [60] C. Gao, C. Zhou, Z. Lin, M. Yang, Q. He, Surface wettability-directed propulsion of glucose-powered nanoflask motors, *ACS Nano* 13 (2019) 12758–12766.
- [61] P.S. Schattling, M.A. Ramos-Docampo, V. Salgueirino, B. Stadler, Double-fueled Janus swimmers with magnetotactic behavior, *ACS Nano* 11 (2017) 3973–3983.
- [62] T. Patiño, X. Arqué, R. Mestre, L. Palacios, S. Sánchez, Fundamental aspects of enzyme-powered micro- and nanoswimmers, *Acc. Chem. Res.* 51 (2018) 2662–2671.
- [63] G. Dunderdale, S. Ebbens, P. Fairclough, J. Howse, Importance of particle tracking and calculating the mean-squared displacement in distinguishing nanopropulsion from other processes, *Langmuir* 28 (2012) 10997–11006.
- [64] R. Golestanian, A. Ajdari, Mechanical response of a small swimmer driven by conformational transitions, *Phys. Rev. Lett.* 100 (2008), 038101.

- [665] S. Hammes-Schiffer, Impact of enzyme motion on activity, *Biochemistry* 41 (2002) 13335–13343.
- [666] E.Z. Eisenmesser, O. Millet, W. Labeikovsky, D.M. Korzhnev, M. Wolf-Watz, D. A. Bosco, J.J. Skalicky, L.E. Kay, D. Kern, Intrinsic dynamics of an enzyme underlies catalysis, *Nature* 438 (2005) 117–121.
- [667] S. Osuna, G. Jiménez-Osés, E.L. Noey, K.N. Houk, Molecular dynamics explorations of active site structure in designed and evolved enzymes, *Acc. Chem. Res.* 48 (2015) 1080–1089.
- [668] L.Y.P. Luk, E.J. Loveridge, R.K. Allemann, Protein motions and dynamic effects in enzyme catalysis, *Phys. Chem. Chem. Phys.* 17 (2015) 30817–30827.
- [669] R. Golestanian, Enhanced Diffusion of enzymes that catalyze exothermic reactions, *Phys. Rev. Lett.* 115 (2015) 108102–108106.
- [670] M. Nakanishi-Matsui, M. Sekiya, R.K. Nakamoto, M. Futai, The mechanism of rotating proton pumping ATPases, *Biochim. Biophys. Acta* 1797 (2010) 1343–1352.
- [671] P.D. Boyer, The binding change mechanism for ATP synthase — some probabilities and possibilities, *Biochim. Biophys. Acta* 1140 (1993) 215–250.
- [672] H. Itoh, A. Takahashi, K. Adachi, H. Noji, R. Yasuda, M. Yoshida, K. Kinoshita, Mechanically driven ATP synthesis by F1-ATPase, *Nature* 427 (2004) 465–468.
- [673] S. Arai, S. Saijo, K. Suzuki, K. Mizutani, Y. Kakinuma, Y. Ishizuka-Katsura, N. Ohsawa, T. Terada, M. Shirouzu, S. Yokoyama, S. Iwata, I. Yamato, T. Murata, Rotation mechanism of enterococcus hirae VI-ATPase based on asymmetric crystal structures, *Nature* 493 (2013) 703–707.
- [674] X. Zhao, K. Gentile, F. Mohajerani, A. Sen, Powering motion with enzymes, *Acc. Chem. Res.* 51 (2018) 2373–2381.
- [675] B. Pelz, G. Žoldák, F. Zeller, M. Zacharias, M. Rief, Subnanometre enzyme mechanics probed by single-molecule force spectroscopy, *Nat. Commun.* 7 (2016) 10848–10856.
- [676] A.S. Mikhailov, R. Kapral, Hydrodynamic collective effects of active protein machines in solution and lipid bilayers, *Proc. Natl. Acad. Sci. Unit. States Am.* 112 (2015) E3639–E3644.
- [677] T. Sakaue, R. Kapral, A.S. Mikhailov, Nanoscale swimmers: hydrodynamic interactions and propulsion of molecular machines, *Eur. Phys. J.* (2010) 381–387. B 75.
- [678] R. Golestanian, T.B. Liverpool, A. Ajdari, Propulsion of a molecular machine by asymmetric distribution of reaction products, *Phys. Rev. Lett.* 94 (2005) 220801–220804.
- [679] C. Riedel, R. Gabizon, C.A. Wilson, K. Hamadani, K. Tsekouras, S. Marqusee, S. Presse, C. Bustamante, The heat released during catalytic turnover enhances the diffusion of an enzyme, *Nature* 517 (2015) 227–230.
- [680] H.S. Muddana, S. Sengupta, T.E. Mallouk, A. Sen, P.J. Butler, Substrate catalysis enhances single-enzyme diffusion, *J. Am. Chem. Soc.* 132 (2010) 2110–2111.
- [681] P. Illien, X. Zhao, K.K. Dey, P.J. Butler, A. Sen, R. Golestanian, Exothermicity is not a necessary condition for enhanced diffusion of enzymes, *Nano Lett.* 17 (2017) 4415–4420.
- [682] J.-P. Günther, M. Börsch, P. Fischer, Diffusion measurements of swimming enzymes with fluorescence correlation spectroscopy, *Acc. Chem. Res.* 51 (2018) 1911–1920.
- [683] J.-P. Günther, G. Majer, P. Fischer, Absolute diffusion measurements of active enzyme solutions by NMR, *J. Chem. Phys.* 150 (2019) 124201–124208.
- [684] Y. Zhang, M.J. Armstrong, N.M. Bassir Kazeruni, H. Hess, Aldolase does not show enhanced diffusion in dynamic light scattering experiments, *Nano Lett.* 18 (2018) 8025–8029.
- [685] A.Y. Jee, K. Chen, T. Tlusty, J. Zhao, S. Granick, Enhanced diffusion and oligomeric enzyme dissociation, *J. Am. Chem. Soc.* 141 (2019) 20062–20068.
- [686] M. Xu, J.L. Ross, L. Valdez, A. Sen, Direct single molecule imaging of enhanced enzyme diffusion, *Phys. Rev. Lett.* 123 (2019) 128101–128106.
- [687] J. Agudo-Canalejo, P. Illien, R. Golestanian, Phoresis and enhanced diffusion compete in enzyme chemotaxis, *Nano Lett.* 18 (2018) 2711–2717.
- [688] R. Golestanian, Anomalous Diffusion of symmetric and asymmetric active colloids, *Phys. Rev. Lett.* 102 (2009) 188305.
- [689] A.-I. Bunea, I.-A. Pavel, S. David, S. Gáspár, Modification with hemeproteins increases the diffusive movement of nanorods in dilute hydrogen peroxide solutions, *Chem. Commun.* 49 (2013) 8803–8805.
- [690] D. Xu, C. Zhou, C. Zhan, Y. Wang, Y. You, X. Pan, J. Jiao, R. Zhang, Z. Dong, W. Wang, X. Ma, Enzymatic micromotors as a mobile photosensitizer platform for highly efficient on-chip targeted antibacteria photodynamic therapy, *Adv. Funct. Mater.* 29 (2019) 1807727–1807738.
- [691] M. De Corato, X. Arqué, T. Patiño, M. Arroyo, S. Sánchez, I. Pagonabarraga, Self-propulsion of active colloids via ion release: theory and experiments, *Phys. Rev. Lett.* 124 (2020) 108001–108006.
- [692] K.K. Dey, X. Zhao, B.M. Tansi, W.J. Mendez-Ortiz, U.M. Cordova-Figueroa, R. Golestanian, A. Sen, Micromotors powered by enzyme catalysis, *Nano Lett.* 15 (2015) 8311–8315.
- [693] X. Zhao, K.K. Dey, S. Jeganathan, P.J. Butler, U.M. Córdoba-Figueroa, A. Sen, Enhanced diffusion of passive tracers in active enzyme solutions, *Nano Lett.* 17 (2017) 4807–4812.
- [694] A. Sitt, J. Soukupova, D. Miller, D. Verdi, R. Zboril, H. Hess, J. Lahann, Microscale rockets and picoliter containers engineered from electrospun polymeric microtubes, *Small* 12 (2016) 1432–1439.
- [695] X. Zhang, C. Chen, J. Wu, H. Ju, Bubble-propelled jellyfish-like micromotors for DNA sensing, *ACS Appl. Mater. Interfaces* 11 (2019) 13581–13588.
- [696] Y.J. Wu, X.K. Lin, Z.G. Wu, H. Mohwald, Q. He, Self-propelled polymer multilayer Janus capsules for effective drug delivery and light-triggered release, *ACS Appl. Mater. Interfaces* 6 (2014) 10476–10481.
- [697] X. Ma, S. Sanchez, A bio-catalytically driven Janus mesoporous silica cluster motor with magnetic guidance, *Chem. Commun.* 51 (2015) 5467–5470.
- [698] J.M. Schurr, B.S. Fujimoto, L. Huynh, D.T. Chiu, A theory of macromolecular chemotaxis, *J. Phys. Chem. B* 117 (2013) 7626–7652.
- [699] X. Zhao, H. Palacci, V. Yadav, M.M. Spiering, M.K. Gilson, P.J. Butler, H. Hess, S. J. Benkovic, A. Sen, Substrate-driven chemotactic assembly in an enzyme cascade, *Nat. Chem.* 10 (2018) 311–317.
- [1000] F. Wu, L.N. Pelster, S.D. Minter, Krebs cycle metabolon formation: metabolite concentration gradient enhanced compartmentation of sequential enzymes, *Chem. Commun.* 51 (2015) 1244–1247.
- [1001] K.K. Dey, S. Das, M.F. Poyton, S. Sengupta, P.J. Butler, P.S. Cremer, A. Sen, Chemotactic separation of enzymes, *ACS Nano* 8 (2014) 11941–11949.
- [1002] G.C. Ilacass, A. Basa, A. Sen, F.A. Gomez, Enzyme chemotaxis on paper-based devices, *Anal. Sci.* 34 (2018) 115–119.
- [1003] F. Mohajerani, X. Zhao, A. Somasundar, D. Velegol, A. Sen, A theory of enzyme chemotaxis: from experiments to modeling, *Biochemistry* 57 (2018) 6256–6263.
- [1004] J. Wang, B.J. Toebes, A.S. Plachokova, Q. Liu, D. Deng, J.A. Jansen, F. Yang, D. A. Wilson, Self-propelled PLGA micromotor with chemotactic response to inflammation, *Adv. Healthc. Mater.* 9 (2020), e1901710.
- [1005] A.-Y. Jee, S. Dutta, Y.-K. Cho, T. Tlusty, S. Granick, Enzyme leaps fuel antichemotaxis, *Proc. Natl. Acad. Sci. Unit. States Am.* 115 (2018) 1–14.
- [1006] A. Somasundar, S. Ghosh, F. Mohajerani, L.N. Massenbunrg, T. Yang, P.S. Cremer, D. Velegol, A. Sen, Positive and negative chemotaxis of enzyme-coated liposome motors, *Nat. Nanotechnol.* 14 (2019) 1129–1134.
- [1007] C. Chen, Z. He, J. Wu, X. Zhang, Q. Xia, H. Ju, Motion of enzyme-powered microshell motors, *Chem. Asian J.* 14 (2019) 2491–2496.
- [1008] S. Nakata, M. Nomura, H. Yamamoto, S. Izumi, N.J. Suematsu, Y. Ikura, T. Amemiya, Periodic oscillatory motion of a self-propelled motor driven by decomposition of H₂O₂ by catalase, *Angew. Chem. Int. Ed.* 129 (2017) 879–882.
- [1009] T. Patiño, N. Feiner-Gracia, X. Arqué, A. Miguel-López, A. Jannasch, T. Stumpp, E. Schäffer, L. Albertazzi, S. Sánchez, Influence of enzyme quantity and distribution on the self-propulsion of non-Janus urease-powered micromotors, *J. Am. Chem. Soc.* 140 (2018) 7896–7903.
- [1010] M. Luo, S.L. Li, J.S. Wan, C.L. Yang, B.D. Chen, J.G. Guan, Enhanced propulsion of urease-powered micromotors by multilayered assembly of ureases on Janus magnetic microparticles, *Langmuir* 36 (2020) 7005–7013.
- [1011] X. Arqué, A. Romero-Rivera, F. Feixas, T. Patiño, S. Osuna, S. Sánchez, Intrinsic enzymatic properties modulate the self-propulsion of micromotors, *Nat. Commun.* 10 (2019) 2826–2838.
- [1012] Z.G. Wu, X.K. Lin, X. Zou, J.M. Sun, Q. He, Biodegradable protein-based rockets for drug transportation and light-triggered release, *ACS Appl. Mater. Interfaces* 7 (2015) 250–255.
- [1013] A. Llopis-Lorente, A. Garcia-Fernandez, E. Lucena-Sanchez, P. Diez, F. Sancenon, R. Villalonga, D.A. Wilson, R. Martinez-Manez, Stimulus-responsive nanomotors based on gated enzyme-powered Janus Au-mesoporous silica nanoparticles for enhanced cargo delivery, *Chem. Commun.* 55 (2019) 13164–13167.
- [1014] C.Y. Gao, Y. Wang, Z.H. Ye, Z.H. Lin, X. Ma, Q. He, Biomedical micro-/nanomotors: from overcoming biological barriers to in vivo imaging, *Adv. Mater.* 19 (2020) 200512–200531.
- [1015] D. Walker, B.T. Kaesdorf, H.-H. Jeong, O. Lieleg, P. Fischer, Enzymatically active biomimetic micropellers for the penetration of mucin gels, *Sci. Adv.* 1 (2015), e1500501.
- [1016] A. Joseph, C. Contini, D. Cecchin, S. Nyberg, L. Ruiz-Perez, J. Gaitzsch, G. Fullstone, X. Tian, J. Azizi, J. Preston, G. Volpe, G. Battaglia, Chemotactic synthetic vesicles: design and applications in blood-brain barrier crossing, *Sci. Adv.* 3 (2017) e1700362.
- [1017] A.C. Hortelao, R. Carrascosa, N. Murillo-Cremaes, T. Patiño, S. Sanchez, Targeting 3D bladder cancer spheroids with urease-powered nanomotors, *ACS Nano* 13 (2019) 429–439.
- [1018] S. Tang, F. Zhang, H. Gong, F. Wei, J. Zhuang, E. Karshalev, B.E.-F. de Avila, C. Huang, Z. Zhou, Z. Li, L. Yin, H. Dong, R.H. Fang, X. Zhang, L. Zhang, J. Wang, Enzyme-powered Janus platelet cell robots for active and targeted drug delivery, *Sci. Robot.* 5 (2020) 6137–6147.
- [1019] Z.J. Chen, T. Xia, Z.L. Zhang, S.Z. Xie, T. Wang, X.H. Li, Enzyme-powered Janus nanomotors launched from intratumoral depots to address drug delivery barriers, *Chem. Eng. J.* 375 (2019) 122109–122120.
- [1020] V.V. Singh, K. Kaufmann, B. Esteban-Fernandez de Avila, M. Uygun, J. Wang, Nanomotors responsive to nerve-agent vapor plumes, *Chem. Commun.* 52 (2016) 3360–3363.
- [1021] I. Ortiz-Rivera, T.M. Courtney, A. Sen, Enzyme micropump-based inhibitor assays, *Adv. Funct. Mater.* 26 (2016) 2135–2142.
- [1022] A.-I. Bunea, I.-A. Pavel, S. David, S. Gáspár, Sensing based on the motion of enzyme-modified nanorods, *Biosens. Bioelectron.* 67 (2015) 42–48.
- [1023] J. Simmchen, A. Baeza, D. Ruiz, M. Jose Esplandiu, M. Vallet-Regí, Asymmetric hybrid silica nanomotors for capture and cargo transport: towards a novel motion-based DNA sensor, *Small* 8 (2012) 2053–2059.
- [1024] Y. Xie, S. Fu, J. Wu, J. Lei, H. Ju, Motor-based microprobe powered by bio-assembled catalase for motion detection of DNA, *Biosens. Bioelectron.* 87 (2017) 31–37.
- [1025] S.M. Russell, A. Alba-Patino, M. Borges, R. de la Rica, Multifunctional motion-color janus transducers for the rapid detection of sepsis biomarkers in whole blood, *Biosens. Bioelectron.* 140 (2019) 154–160.
- [1026] T. Patiño, A. Porchetta, A. Jannasch, A. Llado, T. Stumpp, E. Schaeffer, F. Ricci, S. Sanchez, Self-sensing enzyme-powered micromotors equipped with pH-responsive DNA nanoswitches, *Nano Lett.* 19 (2019) 3440–3447.

- [127] L. Zhao, Y. Liu, S. Xie, P. Ran, J. Wei, Q. Liu, X. Li, Janus micromotors for motion-capture-ratiometric fluorescence detection of circulating tumor cells, *Chem. Eng. J.* 382 (2020), 123041–1230412.
- [128] S. Sengupta, D. Patra, I. Ortiz-Rivera, A. Agrawal, S. Shklyaev, K.K. Dey, U. Cordova-Figueroa, T.E. Mallouk, A. Sen, Self-powered enzyme micropumps, *Nat. Chem.* 6 (2014) 415–422.
- [129] S. Das, O.E. Shklyaev, A. Altemose, H. Shum, I. Ortiz-Rivera, L. Valdez, T. E. Mallouk, A.C. Balazs, A. Sen, Harnessing catalytic pumps for directional delivery of microparticles in microchambers, *Nat. Commun.* 8 (2017) 14384–14393.
- [130] I. Ortiz-Rivera, H. Shum, A. Agrawal, A. Sen, A.C. Balazs, Convective flow reversal in self-powered enzyme micropumps, *Proc. Natl. Acad. Sci. Unit. States Am.* 113 (2016) 2585–2590.
- [131] Y. Zhang, D.A. Gregory, Y. Zhang, P.J. Smith, S.J. Ebbens, X. Zhao, Reactive inkjet printing of functional silk stirrers for enhanced mixing and sensing, *Small* 15 (2019) 1804213–1894222.